

Slip inversion on the creeping thrust fault using geodetic data and repeating earthquakes

Wei Peng¹、Mathilde Radiguet²、Erwan Pathiere²、Kate Huihsuan Chen³

(1)Department of Earth Sciences, National Taiwan Normal University; Institut des Sciences de la Terre in Grenoble, France、(2)Institut des Sciences de la Terre in Grenoble, France、(3)Department of Earth Sciences, National Taiwan Normal University

The Chihshang segment of Longitudinal Valley Fault (LVF) is characterized by both rapid surface creep and creeping at deeper depth. However, the slip inversion of the interseismic creep rate obtained using geodetic measurements does not have a good resolution at depth below 15 km, which indicates that the understanding of along-dip variation of aseismic creep is still very limited. In this study, we apply a static joint inversion that combines both geodetic data (GPS and InSAR) and seismic data (repeating earthquake) to better understand the interseismic creep. By taking advantage of the repeating sequences majorly occurring at depths below 15 km, we are able to explore more about the along-dip variation of aseismic creep. Using the data from 2007 to 2011, our slip model reveals an anti-correlation spatially between the interseismic slip and co-seismic slip of the 2003 M6 event. We also find that the mainshock of the 2003 M6 event occurred on the boundary between areas with high and low interseismic slip. This study provides a new approach of modeling the static creeping behavior, constrained using geodetic and seismic data, which might further improve the time-dependent seismic hazard.

Keywords: interseismic deformation, Chihshang fault, static inversion

Natural and experimental evidence of thermal pressurization and frictional melting during the 1999 Mw 7.6 Chi-Chi earthquake

Wen-Jie Wu¹、Li-Wei Kuo²、Chia-Wei Kuo³、Wei-Hsin Wu¹、

Hwo-Shuenn Sheu⁴

(1)Department of Earth Sciences, National Central University、(2)Department of Earth Sciences, National Central University; Earthquake-Disaster & Risk Evaluation and Management Center, National Central University、(3)Center for Advanced Model Research Development and Applications, National Central University、(4)National Synchrotron Radiation Research Center

Frictional melting and thermal pressurization (TP) can reduce the resistance of fault surfaces and thus govern rupture dynamics and energy partitioning. The hydraulic properties of surrounding rocks, relevant to the efficiency of fluid drainage during sliding, play a critical role in driving either frictional melting or TP in the principal slip zone. Frictional melting and TP have been documented to occur within the principal slip zone of the Chelungpu fault during the 1999 Mw7.6 Chi-Chi earthquake, but the triggering mechanism to which remains unclear. Here, we (1) conduct rotary shear friction experiments on saturated gouges from the Taiwan Chelungpu-fault Drilling Project (TCDP) under varied fluid drainage conditions and (2) compare the experimental products with the principal slip zones of the TCDP. All rotary shear experiments are performed at 1-m/s slip velocity, 18-MPa normal stress, and ~3-m displacement. Scanning electron microscope, focused ion beam-transmission electron microscope, synchrotron X-ray diffraction are conducted for microanalysis. Mechanical data shows that plateau-like peak friction (0.15~0.25) is followed by an ultralow steady-state friction (0.03~0.07) under undrained condition. Peak and steady-state friction are 0.4~0.5 and 0.08, respectively, under drained condition. The formation of distinct shear localization and amorphous materials indicates that frictional melting occurred under drained condition. In contrast, distributed shear and the absence of amorphous materials within the slip zone is recognized under undrained condition. Our experimental observation is consistent with the reported natural observation, suggesting the presence of heterogeneous fluid drainage along the fault zone during coseismic slip. Taken together, we conclude that both frictional melting and TP were operated on gouge because of the variation of fluid drainage and promote the slip in this position during the 1999 Chi-Chi earthquake.

Keywords: frictional melting, thermal pressurization, fluid drainage, Chelungpu Fault, Chi-Chi earthquake

利用曾文溪沿岸階地及碳 14 定年法分析台灣西南部崙後斷層及

口宵里斷層之活動特性

石智偉¹、黃文正¹、波玫琳¹、邱奕維¹、曾雅筑²、劉彥求³

(1)中央大學應用地質研究所、(2)臺灣師範大學地球科學系、(3)經濟部中央地質調查所

崙後斷層與其東側的口宵里斷層位於台灣西南部的台南嘉義一帶，兩者為比鄰的南北走向逆移斷層，前者向東傾，後者向西傾。該區的 GPS 資料顯示跨兩斷層具有每年約 1.5 公分的縮短量，本研究利用流貫本區的曾文溪，其沿岸的階地對比分析，探討崙後斷層及口宵里斷層的活動性及構造關係對此縮短量的可能貢獻。首先利用高精度數值模型進行地形判釋及測繪河階地，再輔以野外調查及 C-14 定年相互對比，並透過地質資料繪製地質剖面，藉以瞭解兩條斷層之關聯與活動特性。本研究根據地形資料分析將階地依相對於現生河道高程的高低分成七階，由高至低分別為 T1 (8 ka)、T2、T3 (3-4 ka)、T4a、T4b(2 ka)、T4c T5，綜合目前所獲得之 C-14 定年結果及前人定年資料，崙後斷層上盤 T4b 階地年代為 1878-1998 cal BP，下盤 T4b 階地年代為 1640-1820 cal BP，且階地高程相似，故推斷崙後斷層可能在 2 ka 以來無活動跡象。口宵里斷層上盤崙後斷層西側的 T3 階地年代為 3820-3446 cal BP，東側的 T3 階地年代則為 3005-3212 cal BP，階地高程差約 20-25 公尺，指示口宵里斷層於全新世內有活動，與其於劉陳尾截切約三千年前形成的階地之證據相符，然而 T3 階地可用定年資料橫跨兩條斷層，因此無法明確得知其抬升量是受崙後斷層或口宵里斷層所主導。為解釋其對於該區的縮短量，本研究綜合上述之野外觀察與定年資料，可得出兩種解釋，其一為崙後斷層因淺部傾角過高而鎖住無法繼續活動，形成口宵里背衝斷層向東逆衝；另一解釋為，因緊鄰崙後斷層西側的烏山頭背斜折曲至臨界點產生破裂，而形成向東逆衝的口宵里斷層，截切崙後斷層並切穿地表河階沉積物。

中文關鍵字：曾文溪、河階地、烏山頭背斜、崙後斷層、口宵里斷層、斷層活動性

泥岩中的斷層帶特性研究：來自車瓜林斷層的見解

陳新翰¹、黃文正¹、邱奕維¹、曾雅筑²、劉彥求³

(1)中央大學應用地質研究所、(2)臺灣師範大學地球科學系、(3)經濟部中央地質調查所

在過往的研究中，有關斷層在泥岩中的產狀特性報導相較為少，本研究以車瓜林斷層為例，對其進行野外地表地質調查、地質剖面清理以及鑽井施作，透過由公釐至公里等級不同中視尺度的觀察，紀錄跨泥質斷層帶的構造變化及特性。車瓜林斷層位於台灣西南部的泥岩區，為古亭坑層中的層間斷層，是一條東北-西南走向現今活躍的左移逆斷層。車瓜林斷層自大廊亭山至千秋寮一帶可以於野外良好追跡約 5 公里，出露寬度約 10-30 公尺，產狀為黃褐色與深黑色泥質條帶所交織的寬帶，顏色上與斷層帶兩側的灰色泥岩有所差異。然而斷層帶中的細部組構在泥岩表面清理的前後有顯著的差異，故本研究選定車瓜林斷層的兩個露頭分別進行地質剖面及鑽井的施作，以剔除斷層帶受地表風化的因子。

地質剖面及鑽井的結果顯示，斷層帶中的變形產狀與岩性相關，我們可以將斷層帶中的岩體區分為三個單元，分別為完整砂岩段、破碎砂岩角礫及含黑色條帶的泥岩。完整砂岩段中破裂面不發達並可見層面；在破碎砂岩角礫，數公釐至數公分的砂質碎片呈角礫狀散佈於泥質基質中；而斷層帶中的泥質岩內則出現寬數公釐的密集黑色條帶狀構造並夾有角礫狀泥質碎屑。於斷層露頭的泥質岩多呈鱗片狀，表面帶有擦痕且破裂面方向具有一致性，將泥質手樣本進行拋光後可觀察到內部夾有大量角礫狀的泥質及砂質碎屑，碎屑長軸呈現具有方向性的排列。在泥岩斷層帶中難以觀察到如脆性斷層帶中變形集中於窄帶的斷層核心及斷層破壞帶，泥岩斷層帶中的變形傾向於相較平均分布於整個斷層帶中，寬度可達數十公尺，然而其中仍存在變形較集中的區域。泥岩中所出現的黑色條帶成因繁多，本研究推測其主要受斷層的剪切作用所形成，但在缺少微觀的觀察狀況下，難以確定其變形機制及礦物組構以探討斷層行為，仍需後續的研究使泥岩斷層帶的構造意義能更加完備。

中文關鍵字：車瓜林斷層、古亭坑層、中尺度地質構造

Inversion of tectonic stress and magma pressures using dikes orientation

Frantz Maerten¹、Laurent Maerten¹、Romain Plateaux²

(1)YouWol、(2)Independent Researcher

In volcano-tectonic regions, stress field variations result from tectonic stress loading and the pressurized 3-D shallow magma chambers. However, the interactions between pressurized magma chambers and tectonic stress remains poorly studied in the context of tectonic stress inversion. Indeed, in classic formulation of stress inversion techniques, which include the inversion of the reduced stress tensor that comprises the stress orientation and stress ratio, it is implicitly assumed that discontinuities cannot open or close, implying that the volumetric part of the regional stress has no influence on the slip direction and magnitude. Therefore, in the case of magma chambers and/or dikes, such classic technic cannot be applied as the volumetric part can no longer be neglected.

In this contribution, we describe a newly developed stress inversion technique that assumes that the heterogeneous stress field around volcanoes, which can be represented by the observed dikes, is a result of the mechanical interaction between the pressurized magma chamber geometry (discontinuities), the traction free Earth surface and the far field tectonic stress. The method, based on the 3-D Displacement Discontinuity Method (DDM thereafter) for homogeneous elastic half-space (successor of Poly3D and iBem3D), automatically finds the optimum far field tectonic stress and magma pressure parameters that best reproduce the observed dikes.

As magma chambers can be regarded as pressurized cavities, DDM results have been validated against known 3D analytical solution for pressurized tube-like cavity. The effectiveness of this stress inversion approach is then demonstrated through natural examples of two different volcanic systems, namely the Spanish Peak (U.S.A) and the Galapagos Islands.

Keywords: stress inversion, geomechanics, excess pressure, magma chambers

蓬萊運動，臺灣是否存在雙碰撞（隱沒）帶？

陳文山¹

(1)臺灣大學地質科學系

古生代以來，臺灣一直位在華夏古陸邊緣，歷經數次板塊聚合事件。因此，代表聚合板塊產物的混同層（*mélange*）更成為瞭解臺灣大地構造演化歷史的重要訊息，尤其代表新生代混同層或傾瀉層的利吉層、墾丁層與玉里帶。但是，當對於 *mélange* 成因或定義有不同的解釋時，就會導致解讀大地構造演化產生很大的差異。如 Lu and Hsü (1992) 認為廬山板岩帶為板塊碰撞產生的混同層，而提出雙碰撞（隱沒）帶模式，認為蓬萊運動歷經了陸（歐亞板塊）—陸（古臺灣地塊；脊樑山脈）—弧（菲律賓海板塊；海岸山脈）的碰撞，潮州與梨山斷層為兩個板塊的邊界；此模式也得到一些迴響。究竟板岩帶是否為混同層（*tectonic mélange*；Hsü (1974) 定義）？哪必須從 *mélange* 定義說起。

Greenly (1919) 首度提出 *mélange* 名詞，當時只是針對岩層產狀的定義為“*block-in-matrix*”，但不具成因的定義。許靖華 (Hsü, 1974) 重塑 *mélange* 定義（義涵了成因的概念），認為位在現今或古老的隱沒帶與造山帶中，此後 *mélange* 一詞才被地質界廣泛應用。而 Silver and Beutner (1980) 將 *mélange* 成因再細分為構造、沉積與衝頂等作用。由於“*block-in-matrix*”產狀經常造成研究者在成因解釋上產生混亂與錯誤解釋，於是 Festa et al. (2010) 又將 *mélange* 成因分為幾種類型：崩積層、斷層帶與聚合板塊邊界的產物；但代表聚合板塊邊界的 *mélange* 須具有一種特性，即含外來的海洋板塊岩塊（*ophiolitic blocks*）。

Lu and Hsü (1992) 認為廬山板岩帶中含有外來的海洋板塊岩塊，但報導地區（寶來、萬大水庫、啞口）出露的火成岩都呈現層間沉積的岩體，屬於板內噴發玄武岩質火成岩，非為外來的蛇綠岩岩塊。依據 Festa et al. (2010) 定義，梨山斷層帶應屬於板塊內斷層（Type 6: *mélange* related to intracontinental deformation）。

晚期中新世以來，蓬萊運動發生弧陸碰撞，玉里帶屬於隱沒帶混同層，利吉混同層屬於碰撞帶混同層，壽豐斷層為歐亞與菲律賓海板塊的隱沒邊界，縱谷斷層為碰撞邊界。

中文關鍵字：混同層、利吉層、墾丁層、蓬萊運動、弧陸碰撞

再論墾丁層形成年代與成因

陳文山¹

(1)臺灣大學地質科學系

墾丁層首先由詹新甫 (1974) 命名，並描述含有外來岩塊，認為是晚中新世造山時期崩積產生的傾瀉層。而墾丁混同層由畢慶昌 (Biq, 1977) 命名，認為在臺灣南部形成雙隱沒帶 (利吉與墾丁混同層)，推測在上-更新世南中國海海殼隱沒產生的。

過去曾於恆春半島進行地質製圖的研究者，皆認為墾丁層與之下石門層或馬鞍山層呈現沉積接觸關係，成因屬於傾瀉層。墾丁層化石研究發現含有上新世 (Huang et al., 1983) 與上-更新世 (黃奇瑜等, 1985; 陳文山, 1992) 時代的化石；但 Pelletier and Stephan (1985) 認為上至更新世化石是污染自鄰近馬鞍山層；認為墾丁層時代應為晚中新世。之後，許多研究者將墾丁層對比至梨山斷層帶的 *mélange* 時 (雙隱沒帶模式)，都是採用墾丁層屬於晚中新世的看法。

本研究團隊利用磷灰石核飛跡年代探討恆春半島造山隆起時期，利用里龍山層砂岩與其中變質砂岩礫石的冷卻年代。由年代已完全被重置的結果，顯示里龍山層沉積之後被埋藏的地溫已高於磷灰石核飛跡定年的封存溫度 ($>135^{\circ}\text{C}$)，推測至少被深埋至 2-4 公里深。磷灰石核飛跡年代為 2.6 至 3.5 百萬年，表示約在晚上新世至早更新世，里龍山層 (恆春半島) 受造山運動影響而開始隆起 (推測地溫略高於 135°C)。因此，從恆春半島造山隆起起始年代來看，顯然墾丁混同層不可能形成於晚中新世，而應在晚上新世至早更新世時期；也印證了墾丁層應是更新世堆積的傾瀉層。而墾丁層也不應該延伸至潮州—梨山斷層，此斷層也不屬於晚中新世的板塊邊界。

中文關鍵字：混同層、傾瀉層、墾丁層、恆春半島、磷灰石核飛跡

臺灣北部脊樑山脈板岩層年代與地體構造演化 -

利用碎屑鋯石鈾鉛定年法

張秋蓮¹、許緯豪¹、陳文山¹

(1)臺灣大學地質科學系

臺灣北部脊樑山脈的大南澳片岩與上覆的板岩層，兩者以不整合（E 礫岩）或斷層接觸，由於化石的缺乏，上覆板岩層的年代仍有爭論。以往認為板岩層的年代最老為中生代，部分學者推測為始新世或中新世。近期的研究顯示不整合面上覆的變質石灰岩層，含有始新世以來的珊瑚化石，顯示不整合面上覆的板岩層，時代應為始新世或年輕於始新世。此外，一般認為臺灣自中生代晚期以來的碎屑性沉積物是由來自西側華南提供的碎屑沉積物推積而成，然而，近期的研究表示 E 礫岩是侵蝕來自東側大南澳片岩和變質花崗岩的碎屑沉積物推積而成。因此，E 礫岩上覆的板岩層的沉積物來源與當時的地體架構是值得重新討論的議題。本研究藉由採集自和平溪上游板岩層中所夾變質砂岩與變質凝灰岩樣本，利用碎屑鋯石鈾鉛定年法，探究板岩層的年代，並藉由碎屑鋯石頻譜討論板岩原岩沉積物的來源，進而描繪古近紀以來臺灣地體架構演變。

利用碎屑鋯石鈾鉛定年法，得到板岩層的碎屑鋯石頻譜結果，分別落在鋯石年齡族群三角圖(ternary diagram)的白堊紀、始新世-漸新世與中新世範圍內，無法呈現確切沉積年代，表示板岩層原岩的沉積物來源不單只源自西側華南，還包括東側大南澳片岩的物源供應。此外，板岩層中所夾的變質凝灰岩層，最年輕峰值為 $32.80 \pm 0.55\text{Ma}$ ，顯示始新世-漸新世時期的張裂活動伴隨著部分火成活動，且板岩層原岩的沉積時代可能始於此時期。綜合碎屑鋯石鈾鉛定年結果，顯示古近紀早期，發生張裂活動，基盤（大南澳片岩和變質花崗岩）形成地壘高區(古中央山脈)，受到侵蝕進而沉積變質礫岩層（E 礫岩），地塹產生納積空間，堆積始新世-漸新世的沉積物，並伴隨著火成岩類活動。古近紀晚期至新近紀早期，整個區域受熱沉陷作用而下沉，堆積中新世以來的碎屑性沉積物。

中文關鍵字：大南澳片岩、E 礫岩、板岩層、碎屑鋯石鈾鉛定年

海岸山脈秀姑巒溪剖面八里灣層之鋯石及磷灰石核飛跡定年研究：

探討源區山脈的剝蝕演化

李政熹¹、陳文山¹、黃奕彰¹

(1)臺灣大學地質科學系

中期中新世以來，海岸山脈從板塊隱沒形成的火山弧，演變為弧陸碰撞的構造環境。前人多針對山脈岩層進行熱定年分析來了解造山帶的時空演化，然而隨著山脈不斷抬升剝蝕，早期出露的岩層已成為碎屑沉積物堆積於盆地中。因此本研究針對海岸山脈秀姑巒溪剖面，採集八里灣層的變質砂岩礫石及砂岩同時進行鋯石核飛跡(ZFT)及磷灰石核飛跡(AFT)定年，輔以砂岩岩象分析，探討脊樑山脈的剝蝕及冷卻歷史。本研究共分析六個變質砂岩礫石及四個砂岩，礫石年代能反映山脈中特定岩層的抬升冷卻歷史，而砂岩年代頻譜則記錄著源區不同岩層的冷卻年代及剝蝕演化。礫石定年呈現兩種結果：(1) AFT~1.8-1.6 Ma 完全癒合、ZFT~3.4-3.3 Ma 完全癒合；(2) AFT~1.8-1.6 Ma 完全癒合、ZFT 部分癒合；代表源區至少有兩種不同變質度的岩層出露。然而，本研究發現某些砂岩的 AFT 完全癒合峰值~4.0-3.0 Ma，老於同層位礫石的 AFT 年代~1.8-1.6 Ma，甚至老於該砂岩的 ZFT 完全癒合峰值，推測此異常的 AFT 年代群應是混合自不同岩層的結果(硬頁岩及板岩)。砂岩的 ZFT 及 AFT 頻譜皆含有大量完全癒合及部分癒合的年代峰值，且隨著地層層序向上，癒合年代逐漸年輕且含量漸增，顯示 1.5-0.8 Ma 期間山脈已出露大範圍極低度(硬頁岩)至低度變質岩(板岩)，層序上亦呈現反剝蝕現象。此外，根據礫石 ZFT 及 AFT 所記錄的冷卻路徑，源區的變質砂岩層於 3.0-1.5 Ma 開始加速冷卻(剝蝕)，與盆地沉積速率加快的時間相近；由砂岩 ZFT 完全癒合峰值計算的山脈冷卻時間亦向上逐漸減少，顯示在 5.2-0.8 Ma 期間剝蝕速率不斷加快，即源區山脈未達到穩定態。

中文關鍵字：核飛跡定年、鋯石、磷灰石、八里灣層、脊樑山脈、剝蝕歷史

利用水璉礫岩的砂岩與礫石之核飛跡定年研究探討上-更新世

脊樑山脈剝蝕歷史

陳彤軒¹、陳文山¹

(1)臺灣大學地質科學系

當山脈碰撞抬升時，造山前緣會逐漸下陷，形成前陸盆地。因此海岸山脈的後前陸盆地於上新世以來持續堆積了厚層的造山帶沉積物，這些沉積物記錄了山脈的剝蝕歷史。本研究目的為利用海岸山脈後前陸盆地的沉積物，以核飛跡定年法研究，探討中部脊樑山脈在造山時期地殼抬升的冷卻歷史，以了解脊樑山脈的剝蝕歷史。本研究的樣本採集自鹽寮坑溪（十號橋），地層為蕃薯寮層和八里灣層，採集砂礫岩層中的變質砂岩礫石和基質的砂岩。蕃薯寮層屬於晚上新世的中-下部深海沖積扇、八里灣層為晚上新世至早更新世深海上部沖積扇，皆來自西側的脊樑山脈。由於前人探討海岸山脈盆地的地溫梯度僅有約 14°C/km，故其核飛跡並不會因深埋作用而被癒合，利用盆地地層中碎屑鋁石和磷灰石的核飛跡年代可以計算脊樑山脈的抬升與剝蝕歷史。

本研究指出蕃薯寮層和八里灣層的磷灰石核飛跡的最年輕峰值介於 6.6 Ma 至 2.1 Ma，越年輕的地層其核飛跡年代也隨之年輕，而鋁石核飛跡皆為部份癒合 (partial annealing)，代表其源區地層並沒受到超過 240 度以上的熱事件。而利用磷灰石和鋁石的核飛跡年代得知於中期上新世開始脊樑山脈的冷卻速率約 52°C/Ma，到了 3 Ma 時再進一步加速冷卻。同時利用磷灰石和鋁石核飛跡可以探討源區的剝蝕岩性，在約 4.4 Ma 時（蕃薯寮層）脊樑山脈開始已經在出露（被剝蝕）極低度變質的硬頁岩岩層，約 3.3 Ma 時（八里灣層）開始出露低度變質岩層（板岩）。

中文關鍵字：核飛跡定年法、剝蝕歷史、海岸山脈、水璉礫岩

A high strain shear zone in the metamorphic core of Central Range, Taiwan: A possible Plio- Pleistocene transform fault

Gong-Ruei Ho¹、Timothy B. Byrne²、Jian-Cheng Lee¹

(1)Institute of Earth Sciences, Academia Sinica, Taiwan、(2)Department of Natural Resources and Environmental Studies, National Dong-Hwa University

The young and presently active Taiwan orogeny provides an excellent tectonic “scene” for studying orogenic processes. In this study, we propose the structures preserved in the Tailuko Belt record oblique, left-lateral convergence, which was mainly driven by the northward movement of the Philippine Sea plate wrt the Eurasian plate. A penetrative foliation, S2, that includes mylonitic and gneissic fabrics, dips moderately WNW and is associated with a sub-horizontal stretching lineation, L2. Hundreds of kinematic indicators from 6 rivers and along-strike transections of relatively high strain are particularly well-developed and include: asymmetric folds, strain fringes around pyrite ore magnetite, S-C fabrics, en échelon veins, R and R’ shears, sigmoidal core-and-mantle structures are identified top-to-southwest sense of shear. In cases where the L2 asymmetry could be determined 80-90% yielded a left-lateral sense of shear. A synthesis of available data suggests that a previously unrecognized zone of strike-slip deformation exists in the Tailuko Belt, and here we document: 1) the distribution of horizontal shear, 2) the kinematics of deformation, 3) the age of deformation and 4) regional consistency between geologic studies and plate reconstructions. We also present a 3D model and discuss the impact of horizontal shear in the shallow structural level of southern Taiwan (e.g., Taimali River and Hengchun Peninsula areas) where previously published kinematic data argue for CCW block rotations. Later deformation events are also recorded in the metamorphic core and cover sequences and are responsible, in part, for tilting of S2 from an initial sub-vertical orientation (Byrne and Chojnacki, this session). Finally, we integrated these field-based observations with data from the Slate Belt and propose that during the development of S2 plate convergence was partitioned into orogen-parallel motion in the Tailuko Belt and orogen-perpendicular in the Slate Belt.

Keywords: Yuli Belt, left-lateral shearing, deformation fabrics, ductile shear zone

以熱變質度解析台灣中部雪山 - 脊梁板岩帶邊界構造運動模式

陳尚謙¹、陳致同¹

(1)中央大學地球科學系

在台灣造山帶中，板岩帶為被動大陸邊緣不同部位沉積物之深埋、隱沒、變質，最終掘升至地表之結果，其中以梨山斷層為界，可再劃分為雪山板岩帶與脊梁板岩帶，二者之地質年代、變形行為、變質度皆有所落差。因此若要對板岩帶，以至於台灣造山歷史有更一步的剖析，作為界線斷層的梨山斷層有不可忽略的研究價值。本研究以拉曼碳質物光譜(Raman Spectroscopy of Carbonaceous Material, RSCM)進行板岩帶變質巔峰溫度(T-peak)高密度量測。RSCM 為一高精度 T-peak 溫度計，其樣本間誤差值可低至 10-15°C，對區域的 T-peak 變化能有更精準的結果。本研究區域於中橫梨山段向北延伸至啞口一帶，界定出雪山-脊梁交界處 T-peak 有約 45-60°C 的陡降。此外預計將 T-peak 結果結合薄片微構造觀察及野外斷層擦痕資料，推論梨山斷層可能的位置、運動模式及變形歷史。

中文關鍵字：拉曼碳物質光譜、梨山斷層、雪山山脈、脊梁山脈板岩帶



從盆地到山脈：整合地層架構與變質沉積岩熱歷史

陳致同¹、張簡婉晴¹、孫浩誠¹、阮氏秋河¹、陳尚謙¹、阮氏金庸¹

(1)中央大學地球科學系

造山帶由海洋隱沒轉進大陸俯衝而形成，洋盆與大陸邊緣上的沉積蓋層經常隨之經歷複雜構造運動並廣泛出露：從山脈外緣褶皺逆衝帶的未變質層序，到山脈內部的變質沉積岩，呈現不同的層序-變質度關係。如此沉積盆地構造反轉的過程反映了造山作用的機制：下覆板塊的岩石材料是於地殼淺部受擠壓即進入褶皺逆衝帶而抬升(前緣加積作用/frontal accretion)，抑或是經歷不同程度的俯衝與構造深埋而後才於深部進入山脈增積體/orogenic wedge (底部加積作用/basal accretion)。藉由詳細比對沉積岩於造山前沉積盆地內的埋藏和其最高變質度，可判定同造山的變質作用的存在與否及強度，指示其進入造山帶的機制；進一步比對褶皺斷層構造中的層位與最高變質度，比較山脈不同部位變形與變質作用的相對年代關係，從而解析合理的底脫面斷層幾何等山脈架構。於東亞地區數個現生與古老造山帶岩石熱歷史分析的初步工作顯示，變質沉積岩是山脈增積體的主要組成，並經由底部加積作用貢獻了大量的地殼增厚，指示了底脫斷層等主要構造的多變與複雜性。

中文關鍵字：岩石熱歷史、增積造山楔、碳物質地質溫度計、台灣造山帶



Extensional tectonics for basement uplift of the Fansipan and Tule mountain ranges in northern Vietnam

Dinh Thi Hue¹、Yu-Chang Chan¹、Chih-Tung Chen²

(1)Taiwan International Graduate Program (TIGP) – Earth System Sciences Program, Academia Sinica and National Central University; Institute of Earth Sciences, Academia Sinica, Taiwan、

(2)Department of Earth Sciences, National Central University

Located in northern Vietnam, the Fansipan and Tule mountain ranges are high topography regions adjacent to the strike-slip Red River Fault, an important structure related to the India-Eurasia collision. How the mountain height is maintained today under humid subtropical climate is important to improve knowledge about tectonic deformations of northern Vietnam and may have broader implications on crustal dynamics of circum-Tibet regions. We therefore utilized observations from the field and digital elevation model (DEM) data, and topographic analyses to constrain active fault systems that likely contributed to the uplift of the mountain ranges. Our observations from DEM and field data indicate possible active normal and strike-slip faults within and surrounding the Fansipan and Tule mountain ranges such as: the Phong Tho-Nam Pia fault, the Tule fault, and the Nghia Lo fault. In addition to these observations, the results from geomorphic indices including both the stream-length gradient index (SL) and the normalized steepness index (k_{sn}) present high values of indices in the footwalls of the inferred normal faults and the low values of indices in the hanging walls. Furthermore, most of identified knickpoints are related to the locations of the mapped faults. The correlation of these data indicates that recent movements of the Fansipan and Tule mountain ranges area dominated by strike-slip and normal faulting under extensional tectonics. We therefore proposed that the extensional tectonics likely play a role for isotactic rebound that maintains the mountain height for a long time in spite of continual erosion in the monsoon-affected areas.

Keywords: Fansipan and Tule mountain ranges, stream-length gradient index (SL), normalized steepness index (k_{sn})

Buchan type metamorphism in the Pingtan-Dongshan Metamorphic Belt, SE China: Evidences from combined EMP monazite and U-Pb zircon ages of mica schists

Jian-Wei Lin¹、Chi-Yu Lee¹、Cheng-Hong Chen¹、Takenori Kato²、
Yuji Sano³、Takahata Naoto³

(1)Department of Geosciences, National Taiwan University、(2)Institute for Space-Earth Environmental Research, Nagoya University, Japan、(3)Atmosphere and Ocean Research Institute, the University of Tokyo, Japan

Detailed age information of the Pingtan-Dongshan Metamorphic Belt in the coastal Cathaysia Block is important in understanding geodynamics of South China continental margin. Geochronological determinations on monazite and zircon inclusions and zircon separates from five mica schists, the most representative rock type in this belt, and two granites intruding schists are studied. Ages of monazite and zircon inclusions within index constituent minerals (quartz, muscovite, sillimanite and K-feldspar) in all schists define a significant peak age at ~100 Ma for the high temperature/low pressure metamorphic event. Along with zircon ages of granites (106 and 101 Ma), a Buchan type metamorphism is proposed regarding heat source from the post-orogenic magmatism in the neighboring igneous province. For discrete zircons, age distribution patterns identify two groups of schist that suggest separated provenances of sediments prior to metamorphism. One group has a simple age cluster (145-130 Ma) inferring proximal Early Cretaceous magmatic rocks in the Cathaysia. Contrarily, another group shows a widespread time span containing two particular age populations of ~1.8 Ga and ~190 Ma that are uncommon in the Cathaysia but comparable to schists in the Tailuko Metamorphic Belt of eastern Taiwan. This suggests an extra provenance between these two belts and a now-concealed microcontinent would play such a role. Accordingly, we advocate a new tectonic framework of this belt that involved two different provenances of sediments and its configuration was influenced by a high temperature regime caused by mantle upwelling as a reflection of slab rollback of the subducted Paleo-Pacific Plate.

Keywords: U-Pb zircon age, EMP monazite age, mica schist, Pingtan-Dongshan Metamorphic Belt, Cathaysia Block

From diagenetic to anchizone, a transition of the very-low metamorphism zones in progressively emerging and exhuming orogen in the southern Taiwan, Hengchun Peninsula.

Jack Giletycz¹、Andrew Tien-Shun Lin¹、Li-Wei Kuo¹

(1)Department of Earth Sciences, National Central University

Southern Taiwan (Hengchun Peninsula) characterizes topography that has been recently emerged above the sea level. Because of that, the surface has been exposed to subaerial process as erosion, landscape reorganization and sediment outflux. As the result, the Hengchun Peninsula might reveal initial exhumation processes and therefore-outcropping first stages of a low-grade metamorphism. Illite crystallinity and X-ray diffraction were used to survey the central and northern Hengchun Peninsula to indicate a potential pattern of this exhumation. 32 samples from sites across the Hengchun Peninsula were collected. Küber Index (KI) derived from the first peak of the FWHM (full-width half-maximum) of the illite diffraction revealed a low anchizone of the very-low metamorphic grade in an asymmetrical pattern shifted to the east. The field structural measurements also show a similar pattern of the advancing deformation from mudstones to argillites exposing pencil cleavage, then slaty cleavage and even first indication of boudinage and crenulation cleavage in the northmost part of the Hengchun Peninsula. These results coupled with a geological map gives a new insight into local geology and tectonic setting of the southern Taiwan.

Keywords: very low metamorphic grade, exhumation pattern, southern Taiwan, Hengchun Peninsula

The clumped-isotope geochemistry of exhumed marbles from the Hoping area, eastern Taiwan

Yi-Chia Lu¹、En-Chao Yeh²、Ling-Wen Liu¹、Thi-Mai Nguyen²、
Pei-Ling Wang³

(1)Department of Geosciences, National Taiwan University、(2)Department of Earth Sciences,
National Taiwan Normal University、(3)Institute of Oceanography, National Taiwan University

The carbonate clumped-isotope thermometer has emerged as an innovative method to constrain the cooling rates and retrograde metamorphic histories of marble. The ‘apparent equilibrium blocking temperature’ recorded by the clumped isotopic composition of marble represents the results of deformation, water–rock reactions, and diffusion-controlled atomic mobility. For a better understanding of the thermal evolution demonstrated by marbles in the Hoping area, a total of 13 calcite marbles were sampled for bulk isotopic ($\delta^{13}\text{C}$ and $\delta^{18}\text{O}$) and clumped isotopic analyses ($\Delta 47$). Grain size, deformation, mineralogy, and element compositions of marbles were also determined via the observation of oriented thin sections, X-ray diffraction analysis (XRD), and energy dispersive spectroscopy (EDS) by Scanning Electron Microscope (SEM). Our results show that the estimated clumped temperatures of calcite marbles in the Hoping area range from 200 °C to 330 °C, which are not correlated with the grain sizes, deformation, and elemental compositions. Noteworthy, the $\Delta 47$ -based apparent temperature of calcite marble experiencing exhumation-controlled cooling rates should range between ~150 °C and 200 °C theoretically, which are lower than the estimated clumped temperatures for the calcite marble in the Hoping area. A plausible magma intrusion event and/or high uplifting rate could cause a higher $\Delta 47$ -based apparent temperature, but a further examination is still needed.

Keywords: Hoping area, marble, carbonate clumped-isotope thermometer

Seafloor crustal deformation and semidiurnal internal tides in northeast Taiwan deduced by GNSS-A measurements

Chi-Hsien Tang¹、Ya-Ju Hsu²、Horng-Yue Chen²、Ryoya Ikuta³、
Motoyuki Kido⁴、Hsin Tung²、Chin-Shang Ku²、Hsuan-Han Su²、
Hsin-Ming Lee²、Yi-Lin Jiang²、Yih-Min Wu⁵

(1)Institute of Earth Sciences, Academia Sinica, Taiwan、Department of Geosciences, National Taiwan University、(2)Institute of Earth Sciences, Academia Sinica, Taiwan、(3)Faculty of Science, Shizuoka University、(4)International Research Institute of Disaster Science, Tohoku University、
(5)Department of Geosciences, National Taiwan University

The dense land-based GNSS network has revolutionized our understanding of earthquake faults in Taiwan; however, due to the lack of offshore data, new tools are needed to address hazards associated with the subduction zone megathrusts and submarine fault systems. Active deformation at subduction zones mostly lies beneath the seafloor and relies on seafloor geodetic techniques. The Institute of Earth Sciences, Academia Sinica, has been developing the Global Navigation Satellite System-Acoustic ranging (GNSS-A) technique and carrying out field tests offshore northeast Taiwan since 2007. In this study, we analyzed the GNSS-A data in 2012-2019 collected at the OILN site, located in the southwestern part of the Okinawa Trough. We optimized (1) the geometry of the seafloor transponder array, (2) the relative displacements for each campaign, (3) the configurations of the shipboard transducer, and (4) the time-variant traveltime delay of the acoustic signal by using a nonlinear inversion. As a result, we extracted the three-dimensional positioning time series and velocities, which broadly agree with the clockwise rotation in northeast Taiwan influenced by the backarc rifting of the Okinawa Trough. Furthermore, the traveltime delay projected to the vertical direction (nadir total delay, NTD) shows a semidiurnal cycle. This feature is compatible with the sound speed profiles measured by CTD during the campaigns, indicating the strong semidiurnal internal tides in the study area. Our analysis shows that GNSS-A measurements are valuable to not only studying seafloor deformation but also physical oceanography.

Keywords: GNSS, acoustic ranging, seafloor geodesy, internal waves

Heterogeneous power-law flow with transient creep in Southern California following the 2010 El Mayor-Cucapah earthquake

Chi-Hsien Tang¹、Sylvain Barbot²、Ya-Ju Hsu¹、Yih-Min Wu¹

(1)Institute of Earth Sciences, Academia Sinica, Taiwan; Department of Geosciences, National Taiwan University、(2)Department of Earth Sciences, University of Southern California

Rock rheology and the interaction between seismic/aseismic slip and viscoelastic flow in the lithosphere control the state of stress and strain over seismic cycles. The rheological behavior of rocks is well constrained by laboratory experiments, but the rheology in natural settings is poorly resolved. These drawbacks highlight the need for a more direct approach to explore rheology in tectonic settings. Here, we designed a kinematic inversion scheme to invert the distributed anelastic strain from geodetic data. Unlike a conventional forward model, our method does not prescribe a rheological model but directly relates surface displacements to off-fault anelastic strain. We explored the lower-crustal rheology in Southern California by using 8 years of GNSS postseismic displacements following the 2010 El Mayor-Cucapah earthquake. Our models image the viscoelastic flow in the lower crust with lateral variations of effective viscosity. A Burgers assembly with nonlinear dashpots ($n=3$) approximates the temporal evolution of stress and strain rate, indicating the activation of nonlinear transient creep and steady-state dislocation creep. The transient and background viscosities in the lower crust of the Salton Trough, where the surface heat flow is locally high, are on the order of $\sim 10^{18}$ and $\sim 10^{19}$ Pa s, respectively, about an order of magnitude lower than the surrounding regions. Our analysis shows the importance of transient creep, nonlinear flow laws, and lateral variations of rheological properties describe the entire history of postseismic deformation following the El Mayor-Cucapah earthquake.

Keywords: seismic cycle, GNSS, postseismic deformation, rheology, Southern California

Toward comprehensive geodetic rate estimation based on TEM fault model

Geng-Pei Lin¹、R. Y. Chuang¹、Kuo-En Ching²、Wu-Lung Chang³

(1)Department of Geosciences, National Taiwan University、(2)Department of Geomatics, National Cheng-Kung University、(3)Department of Earth Sciences, National Central University

Since the island-wide seismogenic structure database and seismic hazard map were published by the Taiwan Earthquake Model (TEM) project, an attempt to incorporate geodetic data into future TEM output was made. We take the advantage of block modeling to estimate slip and deficit rate for the total 45 TEM faults. We build the model in two specific constraints: First, we maintain a uniform model resolution on the fault plane, we put fault nodes in equal distance on each fault. Because previous studies often use to reduce the number of fault nodes due to the expensive computational cost and convenience in setting block geometry. In this version, we set a node interval about 8 km along strike on each fault and at least three layers of node in depth. Second, we use inputs of knowledge-based initial locking ratios (coupling ratio). To gain a realistic model setting, we learn from published literature to set where the asperity was recognized as fully locked, and allow specific surface nodes able to creep when fault creeping was documented. For most cases, locking ratio decreasing along depth is a reasonable and typical constraint. If any fault locking behavior could be non-typical, we remove the depth-dependent constraint and allow the locking ratio on specific fault to be free. With the up-to-date GNSS velocity field, a latest version of slip rate model estimation will be presented. The modeled slip rate and slip deficit rate will be compare to geologic data and discuss the implication of the seismic potential.

Keywords: block model, slip rate, slip deficit, seismic potential

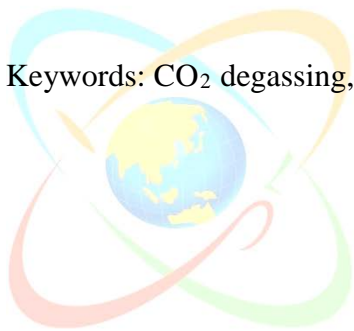
Carbon dioxide degassing around the Chihshang Fault and its implications for exploring earthquake generation process

Ching-Chou Fu¹

(1)Institute of Earth Sciences, Academia Sinica, Taiwan

Measurement of CO₂ degassing at the Chihshang Fault (CSF) in the Longitudinal Valley of eastern Taiwan was performed systematically with a high spatial resolution from a few tens to hundreds of meters. The distribution of CO₂ flux in the area appears as halo anomalies along with the fractures due to crustal leaks. The result revealed that CO₂ flux in the soil gas show anomalous values at the specific positions, and the trace of these anomalous values is coincident with the N-S trending CSF. The flux values of CO₂ in the study area ranged from 0.1 to 26.6 gm⁻²d⁻¹ indicate that faults can facilitate the upward flow of CO₂, with flux rates being greater where the higher densities of fractures occur. Further repeated or continuous measurements of CO₂ flux are critical for improving understanding of the dynamic processes on fault/earthquake generations and seismic activities during the pre-, co-, and post-seismic periods.

Keywords: CO₂ degassing, Chihshang Fault, earthquake generation



迭代邊界回歸面地面點標記法對無人機載光達地面點雲分類的影響

孫正璋¹、詹瑜璋²、張國楨³、江晉霆²、胡植慶⁴

(1)中央研究院地球科學研究所、臺灣大學地質科學系、(2)中央研究院地球科學研究所、

(3)臺北科技大學土木工程系、(4)臺灣大學地質科學系

隨感測器技術進步與小型化，高性能的光達系統可掛載至小型無人機上，相對於以過往空載光達的資料，點雲密度增加超過百倍，可使地形與地上物的測繪更加細緻，但如此綿密的點雲資料已可以觀察到垂直方向上的測量誤差分布，需要不同的演算法來取得地面點雲。

本研究為了處理前述的點雲特性，設計了迭代邊界回歸面地面點標記法，結合使用移動窗格、迭代坡度擬合、地面點雲候選標記等三個步驟，給予每個點評分，在最終以視覺化呈現後，設定一門檻後即可將地面點雲選出。

研究區域選擇宜蘭縣大同鄉梵梵地區，擁有竹針葉混淆林、邊坡、柏油路面、河灘地等多種地形提供分析，以無人機載光達系統並以仿地飛行方式對地區進行測繪，進行標準化的前處理後，即以迭代邊界回歸面地面點標記法對點雲進行標記。

演算法中移動窗格對於不同的地形有明顯不同的表現，本次研究將取兩種地形：混淆林區與邊坡進行演示，設定從 0.5 米至 2 米共三種不同的移動窗格尺寸，對點雲進行標記，並且以不同的門檻值選取地面點雲後，將地面點雲製作成不同尺度的 DEM 呈現。

根據前述流程後處理的結果發現，針對坡度變化不大、有樹林存在的地區，較大的移動窗格對地面點選取的較佳，較可包容因樹木等實體阻擋導致部分區域無測量點的「房屋效應」狀況；而對於短距離內坡度變化較大的地形，則以較小的移動窗格進行分析標記，較可以正確標記坡度變化的邊緣附近的地面點。最終取點的門檻值也對於地形有所不同，針對密林區，因有房屋效應的影響，在過程中特定窗格可能會發生標記錯誤的狀況，但因有移動窗格掃描分析，選用較高的門檻值即可濾除這些不正確標記的點雲；在地形坡度變化較大的地區，則可以降低門檻值，以保留更多邊緣細節。

在移動窗格大小的選取、門檻值選取與處理時間之間取得平衡是重要的課題，未來工作希望對於不同地形特性的點雲資料進一步分析，找出最佳化的參數，提供地形分析、防災、地質判釋等多樣的應用。

中文關鍵字：點雲、地面點雲分類、光達、無人機

無人機光達點雲資料評估及差異分析

陳奕霖¹、張國楨¹、曾俊偉²

(1)臺北科技大學土木與防災所、(2)行政院農委會林業試驗所

近年來由於遙測技術的進步，測量方式由傳統的水準儀及全測站測量一分鐘 3 個點演變至利用雷射掃瞄測距一秒鐘量測數十萬個點的光達技術；以往光達掃瞄儀本體重量且體積大，需要搭配航空飛機執行測量任務，不僅花費時間長、空間上的限制也多，於是發展出能搭載在無人飛行載具(Unmanned Aerial Vehicle)無人機光達，以求更快速且便利的測量，並能夠將空間資料收集的精確及完整，彌補空載光達在細微處辨識不足的地方。

本研究位置位於宜蘭的丸山遺址，使用無人單旋翼直升機 VAPOR55 及無人多旋翼直升機 DJI M600 Pro 分別搭載 RIEGL VUX-1、miniVUX-2 進行光達掃瞄作業。完成掃瞄後首先針對不同光達掃瞄出來的點雲進行空間上的精度評估及分析，探討不同無人機光達之間所存在的差異；而後利用點雲建製數值地形模型，了解無人機光達在使用不同 DTM 製作軟體上所形成的差別。

透過本研究的空間資料取得及分析比較，可以得知不同無人機光達在各無人飛行載具上的特性，針對研究區域提供精確、高解析度之數值地形模型，提供易於判識的地形、地貌，進而評估無人機光達在土地使用概況、維護管理、防災規劃及後續地形差異監測等狀況。

中文關鍵字：無人機光達系統、點雲差異、精度分析、數值地形模型

無人機攝影測量於狹長區域之地形建置精度評估

翁瑋辰¹、張國楨¹、曾俊偉²

(1)臺北科技大學土木與防災所、(2)行政院農委會林業試驗所

無人機的攝影測量與傳統的攝影測量相比可以更有效率且快速的獲得高解析度的遙測影像，然而在於大面積的狹長地形中進行空中三角測量的作業，將會因為地形起伏不同、拍攝時間不同，會形成有連接點匹配不足的問題，位於海岸線的沙灘上更是難以尋找地形特徵點。本研究透過對地面控制點(Ground Control Point)之佈設方法與在於影像上尋找特徵點來建置模型。地面控制點之佈設本研究配合使用虛擬基準站之網路化即時動態定位(Virtual Base Station RTK, VBS-RTK)量測其砂土點位及岸上人工建物之座標，藉此進一步比較正射影像(Orthoimage)及數值地表模型(Digital Surface Model, DSM)，以了解無人飛行載具於狹長地形區域之建模精度並評估誤差。

本研究區域位於苗栗縣竹南鎮至通霄鎮之海岸線，模型之控制點佈設以每500 m 佈設一地面控制點，在航道交界處則於測繪軟體上點選連接點。其中位於竹南縣海岸段之海岸地形砂岸居多，特徵物較少建置之模型之精度較差，而位於後龍段之海岸線則因海角樂園至白沙屯段擁有許多人工建物，而海岸也並非只有單純之砂質海灘，有混合一些卵礫石屬於混合形砂灘，而特徵物比竹南段多因此建置之模型精度較為良好。由本研究可了解影像之特徵共軛點，及地面控制點之佈設對於狹長地形攝影測量之重要性。

中文關鍵字：共軛點、地面控制點、數值地表模型

基於 PPK 技術之無人機攝影測量之地形建模精度評估

陳冠榕¹、張國楨¹、曾俊偉²

(1)臺北科技大學土木工程系、(2)行政院農委會林業試驗所

近年來遙測軟硬體技術不斷演變，無人機的發展也跟著越來越進步，且成本也隨之降低許多，只要使用單點定位無人機搭配地面控制點以及軟體，即可在短時間內取得目標區域內的數值地形模型。而為了在複雜地形建置更精準的模型，差分定位也越來越常使用於無人機上，如使用 RTK 進行實時差分，可以立即取得飛機的精準位置，但本方法容易受地形遮蔽及通訊品質等影響，致使無人機於作業過程中無法直接精確定位。而 PPK 則是使用了後處理差分技術，較不受地形影響，作業半徑大約可延伸至 50km，因此適合用來使用於大範圍的帶狀區域使用，如公路、鐵路等。

本研究之研究區域位於花蓮縣瑞穗鄉吉蒸牧場，拍攝面積約 1 平方公里，測區內地勢平坦且空曠無遮蔽物，飛行及測量條件良好。本研究使用的無人飛行載具分別為 DJI Phantom 4 RTK，以及搭載了非量測性數位相機與外掛 Reach M2 定位模組之 DJI Matrice 600 Pro 多軸飛行器，分別進行了兩期及一期的航拍任務，飛行高度為離地 100 及 200 公尺，並比較以 RTK、PPK，以及使用單點定位等不同無人機定位方式下，不同技術之地形建模精度的差異。研究區現地一共佈設了 33 個地面控制點，控制點測量的部分則使用了 e-GNSS、RTK、以及快速靜態這三種方式進行量測，在進行快速靜態及 RTK 測量時，使用現地的三等衛星控制點作為基站使用。

由於不需要控制點，本研究使用了 30 個點作為檢核點使用，研究成果顯示兩期 P4RTK 在經過後處理解算後，平面誤差分別小於 5.5 公分以及 8.2 公分，而高程誤差小於 7.5 公分，M600 在排除邊界處三個點後，平面誤差小於 7.66 公分，高程誤差小於 10.06 公分。而測量的部分則是快速靜態精度最佳，RTK 次之，e-GNSS 最差；不過由於測區訊號良好且無遮蔽物，因此三種測量方式的較差不會太大。從三種測量方式的較差比較中可以看出，平面部分 RTK 與快速靜態最大較差只有 3.8 公分，e-GNSS 與快速靜態則為 7.9 公分，較 RTK 差；高程部分 RTK 與快速靜態最大較差為 7.8 公分，e-GNSS 與快速靜態則為 8.8 公分，也是 RTK 較佳。

中文關鍵字：無人飛行載具、動態後處理、數值地形模型

運用高精度 LiDAR 數值高程模型輔助區域地質調查 -

以台鐵侯硐崩塌為例

柳鈞元¹、徐文杰¹、黃韋凱¹、李忠勳²、李璟芳¹、紀宗吉³、
林錫宏³、GeoPort 團隊³

(1) 中興工程顧問社、(2) 臺灣大學土木系、(3) 經濟部中央地質調查所

109 年 12 月初台鐵猴硐至瑞芳區間發生岩體滑動災害，大量岩屑材料與風化砂岩層從南北走向的邊坡上向東滑落掩埋台鐵宜蘭線，崩塌範圍呈現節理切割之楔型塊體，滑動塊體上的植生完整地下滑反映著岩體滑動的特徵。參考五萬分之一的雙溪圖幅地質圖，此次岩體滑動恰好位於侯硐背斜軸南翼，地層屬於大寮層下段岩層，層面為 27 度向南南東傾，但現地調查發現當地層面位態多為東北東傾約 15 度，與地質圖記載有所出入。

在沉積岩地區，層面與坡面的空間關係影響岩石邊坡的穩定性，然而五萬分之一的地質圖的尺度並不適用於單一邊坡場址，本團隊藉由高精度 LiDAR 數值高程模型來判釋猴硐地區的岩層跡，嘗試數化追蹤區域內的砂岩分布，並可協助判釋區域的斷層與褶皺構造，輔以現地調查驗證判釋成果。調查成果顯示猴硐地區可數化追蹤岩層跡達 6~12 條，搭配三維地形更可良好地展示侯硐背斜軸部與向東北東傾沒的型貌。

綜整現地調查與高精度數值地形判釋成果，此次台鐵侯硐崩塌的破壞機制較接近平面型滑動，但節理組主控滑動方向與邊界形貌。高精度數值高程模型有助於了解區域地層分布與構造型貌，更可增加現地調查的效率，使地質師與工程師能更全面地了解區域地質概況，降低邊坡場址的地質模型不確定性。

中文關鍵字：LiDAR 數值高程模型、台鐵猴硐崩塌、地質不確定性、岩層跡

使用參考案例建立離散裂隙網路地下水流模型

李在平¹

(1)臺灣電力股份有限公司

台電公司自 1995 年起依法執行用過核子燃料最終處置計畫，目前已完成第一階段我國潛在處置母岩的基本特性調查，並參考瑞典核燃料及廢棄物管理公司 (Swedish Nuclear Fuel and Waste Management Company, SKB) 所發展的 KBS-3 處置概念，以研究用參考案例的方式發展處置相關安全評估技術，於 2017 年提交「我國用過核子燃料最終處置技術可行性評估報告(SNFD2017 報告)」，並通過國際同儕審查。由於參考案例的處置母岩屬於較不透水的結晶岩體，本研究採用近年發展中的離散裂隙網路(Discrete Fracture Network, DFN)模型建置一簡化之區域地下水流模型，與 SNFD2017 報告中的分析結果進行比對。使用資料主要來自六口深度約 500 m 之鑽井以及地表測繪，裂隙分析統計則主要依據孔內地球物理井測與岩心紀錄。由於參考案例過去並未執行高精度之孔內水力試驗，缺乏對應離散裂隙網路模型所需之岩體透水關係式，本研究參考瑞典 Forsmark 花崗岩的現地調查數據，假設裂隙半徑與導水係數具半相關(semi-correlated)的冪律關係。模型全域共生成約 2100 萬個離散裂隙後，除了處置設施周圍保留 DFN，其他部分則使用升尺度方法轉換為等效孔隙介質(equivalent continuous porous medium, ECPM)進行地下水流分析，並選定一截切處置孔之導水裂隙進行質點追蹤，分析其向外的可能傳輸路徑。研究結果顯示區域地下水流的模擬結果與 SNFD2017 報告相近，採用混和 DFN 與 ECPM 的方法，是未來研究後續安全評估所需地下水流與傳輸途徑之可行方式，但尚需要搭配現地高精度的地層透水性試驗才能降低模型的不確定性。

中文關鍵字：裂隙岩體、離散裂隙網路、地下水、安全評估

台灣斷層破裂至地表機率模型之建置

張志偉¹、張毓文¹、趙書賢¹

(1)國家地震工程研究中心

當中大規模的極淺地震發生時，其所引致之地表破裂將造成地上建物或橋梁損壞，例如 1999 年集集地震及 2018 年花蓮地震，部分橋樑及建物均因地表錯動而造成嚴重損傷。有鑒於此，錯動量是為耐震設計重要參考。因地震引致之錯動量，除以經驗式直接進行估算外，亦可採用機率式斷層錯動量危害分析 (Probabilistic Fault Displacement Hazard Analysis, PFDHA)。在進行機率式分析時，須了解地震發生時是否引致地表破裂，機率為何，以評估鄰近斷層之工址，在特定的地震回歸期中，計算可能的地表斷層錯動量，做為日後重要設施地震影響之評估。本研究將應用台灣歷史地震紀錄，發展斷層破裂至地表機率模型，提供機率式分析之參考。

利用中央氣象局於 1900 年以來規模 5.0 以上、深度小於 20 公里之地震目錄，以及 Taiwan Earthquake Model 於 2015 年所公布台灣陸上 38 條活動斷層之位置，利用震央分佈與斷層跡線之相對位置，將台灣陸上可能與斷層活動有關的地震事件篩選出。除此外，本研究蒐集中央氣象局 1901-2000 年的災害性地震列表 91 筆地震事件(<https://scweb.cwb.gov.tw/zh-tw/page/disaster/5>)、台灣十大地震災害地震圖集、中央地質調查所特刊與其他文獻資料，依其對於地震災害的文字描述與災情嚴重程度，篩選因斷層錯動而造成地表破裂的地震事件。綜合上述兩組地震資料庫，區分出屬於斷層地震且有破裂至地表以及未破裂至地表之事件，再利用「邏輯迴歸模型」(Logistic Regression Model)(Hosmer and Lemeshow, 1989)建置屬於台灣本土陸上斷層破裂至地表的機率模型，此機率模型會與震源相關參數有關，如地震規模、震源深度與震源機制解等。地震規模越大、震源深度越淺，則代表斷層破裂至地表的機率越大。

本研究建立與地震規模有關的破裂機率模型，且不對各事件進行震源機制解的分類，將陸上所有斷層與所有地震事件視為一體。機率模型所得到的初步成果為：若台灣地區陸上發生一顆規模 6.5 且深度小於 20 公里的地震，其斷層破裂至地表的機率為 37.3%；若規模 7.0 且深度小於 20 公里的地震，其斷層破裂至地表的機率則為 74.0%。

中文關鍵字：邏輯迴歸模型、條件機率模型

深開挖基礎與上覆土層受正斷層錯動之影響

方儒雅¹、林承翰¹、林銘郎¹

(1)臺灣大學土木工程學系

近年的地震事件顯示除了強地動之外，斷層錯動造成的同震地表變形也是斷層附近結構物產生破壞的原因。台灣人口稠密，建物用地無可避免的會與斷層帶有交集，例如屬正斷層的山腳斷層鄰近台北盆地，斷層帶上有許多高樓結構物使用筏式基礎搭配連續壁(即深開挖基礎)，連續壁向下延伸增加了土層與基礎互制行為的複雜性，此複雜性又進一步加深了量化評估筏式深基礎與上覆土層受正斷層錯動之影響的難度。

為有效降低斷層錯動可能形成的災損，本研究使用基於有限差分法耦合離散元素法的三維數值模型，離散元素法模擬受正斷層錯動下產生應變集中帶的上覆砂土層，有限差分法則模擬筏式基礎結構物因斷層錯動和地表變形產生的反應。為了確認此耦合分析方法能合理模擬上述複雜課題，本研究建立三個基本案例模擬與理論解比較，也進行一系列的縮尺砂箱實驗與數值模擬結果相互校核，最後透過真實案例模擬來確認分析方法能合理地應用於全尺度現地案例。

基礎中心與斷層尖端之相對位置為本研究之主要變因，結果顯示位在斷層尖端上方的基礎由於為三角剪切帶所包圍，會產生明顯的位移並傾斜，斷層影響範圍增加並在兩側出現主、被動破壞；當基礎與斷層尖端保持適當距離時，基礎則沒有明顯變形且可有效阻擋三角剪切帶發育。根據當前研究城成果，本研究建議在設計結構物配置時若無法保持距離，靠上盤側配置能受較少影響，並採取適當調適措施，減少其受地表變形之損害。

中文關鍵字：正斷層、同震地表變形、土壤與基礎互制、深開挖基礎、耦合有限差分法與離散元素法

Multiple-segment rupture and earthquake probability in fault system

Chung-Han Chan¹

(1)Earthquake-Disaster and Risk Evaluation and Management (E-DREaM) Center, National Central University; Department of Earth Sciences, National Central University

Several seismic events are attributed to ruptures on multiple seismogenic structures during coseismic periods. Their instantaneous ruptures along large structures patches generate earthquakes with large magnitudes, resulting in fatality and damage. Thus, this study aims to understand interaction between seismogenic structures through identifying potential structures that could rupture instantaneously in a coseismic period and assessing seismic hazard. For such purpose, triggering interactions between seismogenic structures will be discussed through the Coulomb stress model; earthquake probability will be quantified using both statistics- and physics-based approaches through the Gutenberg-Richter relationship and the rate-and-state friction model, respectively. In order to evaluate their credibility, these models will be applied in the earthquake cases, including the 1935 Hsinchu-Taichung earthquake. Based on the multiple-structure system database summarized through this proposal and distribution of recent earthquakes, dynamic seismic hazard map platform that could be revised in real time will be proposed, beneficial to both subsequent researches and promotion of popular science.

Keywords: Earthquake probability, seismic hazard assessment, Coulomb stress change, Gutenberg-Richter law, rate-and-state friction law, scaling law

假戲真做古海嘯

齊士崢¹、施雅軒¹、顏君毅²、陳佳宏¹

(1)高雄師範大學地理學系、(2)東華大學自然資源與環境學系

學者依據「臺灣采訪冊」「祥異」記載的「加藤港暴漲」，及相關數學模式模擬，認為南部地區可能發生 5 公尺以上的海嘯。「加藤港暴漲」發生於乾隆 46 年 (1781)，是由嘉慶元年 (1796) 錄取的恩貢生林師聖於道光 10 年 2 月 20 日 (1830) 所報。傳世的「臺灣采訪冊」是傳抄本，原始版本已經亡佚。林師聖是臺灣縣人，雖生卒時間不明，但仍可推測災害事發 49 年後才經採訪、記錄，而沒有發生當時官方記錄的「加藤港暴漲」事件，極有可能發生於他的幼年時期之前，而他後來是聽聞自當事人、目擊者，或是輾轉聽聞的鄉野奇譚，均未說明。不過可以確定的是乾隆 46 年時高雄、屏東平原已經納入清帝國鳳山縣治理，加藤港始終屬於「港東里」，直至日治時期亦從未劃分於「港西里」，當然更跟「鳳港」或「西里」無關。再由文獻與古地圖資料分析，「加藤港」是河口港，位於現在的東港、林邊之間，乾隆年間是港東里的重要港口，所以「港有船通郡」。不過「加藤港」至道光年間因河川改道、港灣淤積而消失了。至於「加藤港暴漲」記載的「水漲數十丈」，若非筆誤就是指稱水平距離，絕非高度。會被認為是兩波波高分別是 3 至 5 公尺海嘯，則是學者對於報導中「嗣聞是日」發生的另一個現象的一廂情願詮釋。以當代對海嘯破壞力的理解，人攀援木竹、茅草屋頂而至尾，或在搖曳的竹上避難，應該沒有機會在 3 至 5 公尺的海嘯中全體存活。「加藤港暴漲」的疑點實在太多，因嚴重的災害而喪命的竟然是一位「不孝悍婦」，能夠被傳說、記錄，不可忽視的重要原因恐是緣於其規訓婦女的隱喻意義。謠言現象不是今日才有，脫離現實的記載早應該認定為不實傳言的假新聞而以結案處理，實在無需如此費盡心思地牽強附會、擴大恐懼。不過「加藤港暴漲」是海嘯的真偽與高屏海岸是否曾經發生海嘯純屬不同議題，全世界的海岸也當然都有面臨海嘯災害的可能性，但「可能性」與「事實」不同，「面臨海嘯災害」不應該是問題的核心，「可能性」或者「風險」才是重點。高屏海岸是否有古海嘯地質記錄和未來面臨的「海嘯風險」，是更需要進一步研究和確認的主題。

中文關鍵字：臺灣采訪冊、加藤港暴漲、古海嘯、風險

太平地區車籠埔斷層的時空變化與在地球科學教育上的運用

鍾令和¹、黃豐昌²、陳榮原²

(1)國立自然科學博物館車籠埔斷層保存園區、(2)臺中市立建平國小

藉由持續觀察 20 年在太平地區 921 集集地震破壞的時空變化，將其歸納整理，分成四種類型：1. 地震破壞的演變 2. 斷層抬升 3. 地震相關的地質災害 4. 建築物的破壞與後續處理四大類。將這些災害的負面遺產融入鄉土教育與戶外教育課程，並配合車籠埔斷層保存園區與 921 地震教育園區的資源進行課程設計。藉此讓沒有經歷過規模七地震的新生代學生了解台灣的宿命，並進行相關的防救災知識與訓練，進而為下一次的大地震預作準備。

中文關鍵字：集集地震、車籠埔斷層、太平



災防科學，鍊結國際-「智慧災防新南向」

計畫報告

鍾孫霖¹、張文彥²、黃韶怡¹

(1) 中央研究院地球科學研究所

(2) 國立東華大學自然資源與環境學系

呼應政府新南向政策，經由整體執行「智慧災防新南向」，增進台灣防災科技於區域內的影響力，透過災防科技之應用落實，協助新南向國家提昇防災與減災能力。並重新定位我國在亞洲發展的重要角色，以打造臺灣經濟發展的新模式，創造未來價值。為有效配合政府新南向政策，智慧災防新南向執行推動辦公室自 2018 年 8 月開始統籌及協調三大面向進行：「建置維運新南向國家整合式災害情資決策系統與智慧防震技術輸出計畫」，「南海雙島國際大氣及海洋科學觀測平台與合作研究計畫」及「新南向國家地球科學重點科技合作研究深耕計畫」。為因應我們面臨的區域性及全球性的威脅，例如全球暖化、氣候變遷以及地震、火山、海嘯和颱風豪雨等自然災害的影響，世界國家皆著眼於尋覓適當的國土調適策略及智慧防災作為。智慧災防新南向計畫自 107 年八月執行至今，除持續原有交流計畫之合作夥伴以外，已陸續與新南向國家之學術機構簽署合作備忘錄，內容涵蓋互訪協議(研究人員及學生)、境外研究中心設立、雙邊教學暨短期課程協議、雙邊國際會議協定，以及跨國合作計畫執行等等項目，並積極培訓及延攬人才，進行雙邊會議及工作坊、野外調查的移地研究、人員互訪學術交流，進一步落實學術發表及產學合作。

中文關鍵字：新南向計畫、東南亞、減災、南海、東沙環礁、太平島

英文關鍵字：New Southbound Program, Southeast Asia, Disaster risk reduction, South China Sea, Dongsha Atoll, Taiping Island

Status of the Taiwan-Philippines collaboration under the New South Bound Project

Shu-Kun Hsu¹, Shiou-Ya Wang², Yi-Ching Yeh¹ and Ching-Hui Tsai²

¹ Department of Earth Sciences, National Central University, Taiwan

² Center for Environmental Studies, National Central University, Taiwan

The main purpose of our Taiwan-Philippines collaboration on earth sciences is better understand the tectonics and seismic hazard of the Manila subduction zone. The Manila subduction zone extends from south Taiwan to the Mindoro Island of the Philippines. Both ends of the Manila subduction zone are undergoing a collision between the Philippine Sea Plate and the Eurasian Plate. The Manila subduction zone is considered as a potential place to generate large earthquakes and tsunamis that could jeopardize the coastal areas around the South China Sea. However, the tectonics of the Manila subduction zone was not well known because of the lack of seismic stations off the west Luzon Island. In this project, we planned to deploy 30 OBSs (Ocean Bottom Seismometers) along the Manila Trench, so that we can record one year earthquake data and better understand the velocity structures of the lithosphere of the Manila subduction zone. Unfortunately, due to the Covid-19 pandemic, our plan was postponed to March-April 2022. To fill the project gap, we had planned a transitional cruise to study the seismic structures of the northernmost Manila subduction zone. For that, we have deployed 18 OBSs off south Taiwan in November 2020 and 15 OBSs were recovered in October 2021. This earthquake data set is quite unique because the earthquake data, for the first time, provide us a wonderful coverage of the seismic ray paths and allow us to better understand the tectonics of the initial collision of the Taiwan orogen. It also provides us a better opportunity to examine the seismic hazard of the southern Taiwan, especially along the deformation front. Here, we will show the very preliminary results from the OBS data.

推動新南向國家整合式災害情資決策系統之建置與維護

李維森(1), 陳宏宇(1), 吳逸民(2), 蘇文瑞(1), 劉怡君(1), 陳可慧(1), 張芝苓(1), 李燕玲(1)

(1) 國家災害防救科技中心

(2) 國立台灣大學地質科學系暨研究所

自 2018 年 7 月起由科技部支持，在推動新南向國家整合式災害情資決策系統之目標下，分四期推動下列工作：(1) 增設現地型地震 P 波感測儀，逐步建立相關國家地震基本資料收集；(2) 建立當地客製化之災害情資網，以期協助災害情資彙整與災害衝擊評估；(3) 增設微型氣象站，以進行多重災害之監測；(4) 結合國內產業依據當地的需要，輸出智慧型防災監測系統；(5) 應用臺灣防災科技與應用成果，協助培訓相關國家防災管理體系與能力建構。這個計畫是基於臺灣歷年在防災上之知識創新、實際經驗與產品開發，透過本計畫之落實可以結合科學研究與國際平台之實質輸出，拓展與東協及南亞等國家的關係，進而強化區域交流發展與合作。同時也打造臺灣防災知識之經濟輸出的新模式，並重新定位我國在協助亞洲發展的重要角色，創造未來價值。至 110 年 8 月，本計畫已經與菲律賓、印尼、越南、泰國、印度、不丹、馬來西亞、尼泊爾、阿拉伯聯合大公國與紐西蘭等 10 國進行接觸與討論，已完成簽署 8 項合作協議(菲律賓 2 項、不丹 1 項、尼泊爾 2 項、印度 1 項、阿拉伯聯合大公國 1 項、越南 1 項)及 1 項合作落實計畫書(越南)，實地在菲律賓馬尼拉及怡朗市、不丹皇家大學與尼泊爾 7 城市完成多點智慧防災監測設備建置、進行相關防災軟硬體教育訓練，並已實際接收多筆即時災害情資作為後續防災資料庫及防災情資分析之基礎。

中文關鍵字：新南向政策, 智慧型防災監測系統, 能力建構

英文關鍵字：New Southbound Policy, Smart Disaster Risk Management, Capacity Building

建置維運新南向國家整合式智慧地震防災技術輸出

周中哲*、柴駿甫、黃世建、陳家漢、蕭輔沛、王仁佐、黃靖閑

財團法人國家實驗研究院國家地震工程研究中心

近年南向諸國正值經濟起飛，擴大推動基礎建設之際，對於基礎建設相關人才與技術需求孔急。國家實驗研究院國家地震工程研究中心長期發展地震工程防、減災技術，累積豐碩成果，配合近期政府積極推動之新南向政策，期能結合產、學、研能量共同合作，透過地震防災技術輸出，提供南向諸國所需之地震防災相關技術，協助南向諸國提升地震防災能量。

計畫主要的工作項目：(1)與產業合作輸出地震防災技術：與國內防災產業合作，由國震中心協同國內業者一同赴南向諸國拜會、技術推廣，並與當地政府與民間機構洽談，以於當地擇定合適標的（建物、工業區或重要設施等），協助提出地震防災解決方案並進行技術輸出，後續並以此作為示範場域，作為未來當地技術推廣之基礎。(2)舉辦短期國際訓練班培訓南向國家專業人士：培訓南向諸國人士，協助提升該國地震防災技術能量外，亦從中推廣國震中心成果，加速未來技術輸出海外的機會。

目前地震預警系統已在印度、紐西蘭等國建置示範站，校舍評估與補強技術也在今年在泰國完成三棟補強示範案例，國際耐震相關訓練班也在台灣、印尼、菲律賓、泰國等國舉辦且獲得當地產業界熱烈迴響，相關成果與未來規畫將在文中報告說明。

中文關鍵字：新南向計畫、智慧防震技術、地震預警系統、國際訓練班

英文關鍵字：New Southbound Policy, intelligent seismic technology, earthquake warning system, tomography, international training program

東沙環礁三大死相

宋克義¹，高宏明¹，傅科憲^{1,2}，黃湘倫¹，張海璿¹

1 國立中山大學海洋科學系

2 現職:國家海洋研究院

東沙環礁位處南海，距離最近的大陸有幾百公里，儘管如此，過去幾年發現三大死亡現象，分別是礁台海草床大量死亡，潟湖內珊瑚大量白化，以及潟湖東邊魚類大量死亡。其中海草床大量死亡因為利用衛星影像都可以觀察到，估計的範圍和開始的季節最為準確，大約是25平方公里，引發的原因可能是夏天缺氧加上高溫，目前有些受損的海草床在恢復中，有些則仍然在持續惡化，根據衛星歷史影像這是2014以前東沙環礁所沒有發生過的。潟湖中珊瑚的白化經常導致死亡，這主要是在夏天由高水溫所引起，影響的範圍可能用無人空拍機估計，在1980年以前全世界沒有任何珊瑚礁大量白化現象的報導。此外，東沙環礁魚類的大量死亡發生在五六月潟湖東邊，可能是海水的分層和缺氧導致，由於發生的深度大約在15公尺水深，是目前觀察和研究最為困難的現象。

南海國際科學研究設施建置與管理 東沙島與太平島研究站和南海氣象建置成果

林博雄¹ 宋克義²、詹森³、劉千義⁴、周昆炫⁵

¹臺灣大學大氣科學系 ²中山大學海洋科學系 ³臺灣大學海洋研究所
⁴中研院環境變遷研究中心 ⁵文化大學大氣科學系

本研究總結科技部「南海國際科學研究設施建置與管理」四年計畫的科學研究站建置以及島上的氣象資訊四年統計和南海地區的閃電和降水的空間特徵。本計畫在 2018 年年末分別在太平島碼頭以及東沙島瀉湖賞鳥小屋設立學研究站設備(貨櫃)。原期待四年可以逐步擴增強化太平島國際聯合研究站規模，無奈 2020-2021 年 COVID-19 疫情不僅影響國際交流，也造成登島船班限制與船位的影響，不過本計畫在前兩年(2018-2019)穩定在 5 月和 12 月登島進行密集性探空氣球施放，並將資料分享給台灣季風研究和國外同期的 YMC 和 PISTON 國際觀測實驗；原定在東沙島建立大氣與海洋海空無人載具測試基地(sandbox, 沙盒)也因為南海軍情緊張和東沙島跑到改建工程進行而叫停。2019 年透過海科中心勵進號研究船南海首航串起東沙島、太平島兩島嶼和台灣本島的探空觀測點形成南北觀測測線。也在新海研一號和新海研二號研究船進行氣象探空設備和海上航次。為未來的研究船藍海策略建立實作基礎設施和甲板操作經驗。

兩島四年的地面氣象資料建構島上環境觀測的基本資訊(風場和雨量特徵)，特別是颱風過境島上的極端天氣，將有重點說明，這些資料連同南海周遭國家重電氣象站都收錄在資料庫，將在計畫結束後(2022 年)全數轉移到大氣學門資料庫。

此外本計畫所收錄南海地區閃電以及 GPM 衛星的降水資訊和對流雲位置也都逐日記錄完整，可以季節和全年平均來呈現南海大氣特色。由於太平島特有關鍵性地理空間，能有效支援季風和島嶼熱對流研究、海洋大氣耦合研究、海洋環境生態研究、閃電監測、電離層大氣研究(地磁赤道通過帶)等國際型議題 並突顯我國與南海周邊國家和平共處理念，並經由兩島嶼的科學研究站經營(監測應用)與科學資訊分享，來明確宣示台灣在南海領土主權以及與國際合作接軌的用心。本計畫也參與另一整合型計畫(台大大氣科學系隋中星教授主持之雲、輻射、海-氣邊界層過程和南海季風，三篇文章送審)及和產出期刊文章 8 篇。太平島研究站設施將移轉到海洋委員會國家海洋研究中心繼續推動。

新南向國家地球科學重點科技合作研究深耕計畫-南海計畫

**Comparative Phylogeography and Phylogeny of Pennah Croakers
(Teleostei: Sciaenidae) in Southeast Asian Waters**

陳韋仁¹、Hong-Chiun Lim^{1,2}, Ahasan Habib^{3,4}

¹國立臺灣大學 海洋研究所

² Department of Biotechnology, Faculty of Applied Sciences, AIMST University, Kedah, Malaysia

³ Faculty of Fisheries and Food Science, Universiti Malaysia Terengganu, Terengganu, Malaysia.

⁴ Department of Fisheries and Marine Science, Noakhali Science and Technology University, Noakhali, Bangladesh.

A broad-scale comparative phylogeographic and phylogenetic study of pennah croakers, mainly *Pennahia anea*, *P. macrocephalus*, and *P. ovata* from Southeast Asian waters, was conducted to elucidate the mechanisms that may have driven the species/genetic diversification of marine organisms in these waters. A total of 316 individuals from the three species, and an additional eight and six individuals of *P. argentata* and *P. pawak* were employed in this study. Two genetically divergent lineages each of *P. argentata* and *P. anea* (lineages L1 and L2) were respectively detected from the analyses based on mitochondrial *cytochrome b* gene data. Historical biogeography analysis with a multi-gene dataset revealed that *Pennahia* species most likely originated in the South China Sea and expanded further into the eastern Indian Ocean, East China Sea, and northwestern Pacific Ocean through three separate range expansion events. The main diversifications of *Pennahia* species occurred during Miocene and Pliocene periods, and the occurrences of lineage divergences within *P. anea* and *P. argentata* were during the Pleistocene, most likely as a consequence of cyclical glaciation events. The population expansions that occurred after the sea level rise might be the reason for the population homogeneity observed in *P. macrocephalus* and most *P. anea* L2 South China Sea populations. The significant structure observed between the two populations of *P. ovata*, and the restricted distributions of *P. anea* lineage L1 and *P. ovata* in the eastern Indian Ocean, might have been hampered by the northward flowing ocean current at the Malacca Strait and by the distribution of coral reefs or rocky bottoms. While our results support S. Ekman's center-of-origin hypothesis taking place in the South China Sea, the Malacca Strait serving as the center of overlap is a supplementary

postulation for explaining the present-day high diversity of pennah croakers centered in these waters.



東沙海草床之生地化循環與微生物之關係及其受全球環境變遷之影響

洪慶章¹、陳慶能¹、王志騰¹、黃蔚人¹、塗子萱¹、袁中新²、
周文臣³、施詠嚴⁴

1. 國立中山大學 海洋科學系
2. 國立中山大學 環境工程研究所
3. 國立台灣海洋大學 環境與生態研究所
4. 海軍軍官學校

東沙島環礁擁有世界級的原始海草床生態系與生物多樣性。近年來東沙海域受全球環境變遷(如暖化或酸化)的衝擊，尤其是在東沙內環礁的水域內，其對海草床、珊瑚礁與海洋生態系的威脅可能要比其他深水海域來的顯著且嚴峻。特別是 2020 年東沙環礁內(水深 15 米)之夏季缺氧現象有逐漸惡化的趨勢，而發生在 2014 - 2015 年間的大規模海草死亡事件，目前也原因不明。初步的研究結果顯示環礁內之夏季缺氧現象主要可能是肇因於海水溫度升高、風浪變小及海水流動減緩與大量掉落之海草葉，待這些有機物分解後及海水流動增強，海水的缺氧現象就會消失。此外本研究也發現東沙島之微生物呼吸作用，可能會降低碳酸鹽飽和度，從而推動碳酸鹽溶解並導致鹼度提高，從而在碳酸鹽化學系統中形成這種獨特的沉積模式。這一發現顯示沿海藍碳生態系統可以緩衝海洋酸化和吸收大氣二氧化碳的潛力，特別是在半封閉環境中，通過代謝碳酸鹽溶解來增加鹼度的重要性。最後我們也會報導東沙島海草床之營養鹽供應、溫室氣體(CO₂、CH₄、N₂O)通量、海草生產力及分解速率、沉積物間隙水之硫化學的特性及微生物與細菌對有機物質(主要是碳、硫)降解之角色。

珊瑚礁地下水與營養鹽傳輸對東沙環礁底棲生態影響

陳建勳¹、黃婷萱¹、陳世明¹、劉名允¹、王豐寓¹、郭孟穎¹、曾瓊蓉¹、
劉莉蓮²、王兆璋¹

1 國家實驗研究院台灣海洋科技研究中心

2 國立中山大學海洋科學系

本計畫探討地下水與營養鹽傳輸對東沙環礁底棲生態的影響，由於海底地下水滲流在過去十年間被認為是會發生在全球陸棚的現象，是陸海交換的一個重要因子，先期的觀測紀錄在東沙環礁潟湖海底，紀錄到比正常海水鹽度、溶氧及 pH 較低的海水環境，推測海底地下水不只存在珊瑚島，也存在於環礁潟湖底下。因此本計畫預期採集東沙島及環礁潟湖的孔隙水及滲流地下水，分析營養鹽及其他水質參數，並結合模式及底碇觀測，推估珊瑚島礁海底地下水滲流後的擴散影響範圍，及其對珊瑚島礁底棲生物生態的可能影響。

本年度的研究工作包括以頻譜分析先期的觀測資料，以及今年 8 至 9 月間的東沙環礁海域調查觀測；初步結果顯示先期的觀測存在有異於正常海況的現象，其海水鹽度降低頻率大約每 24 小時一次，推測是較低鹽度的地下水滲流，再受到潮流影響，將穿越礁台往外礁擴散。本年度的海域調查著重於底質調查、底水及滲流水的水質特性及水體氬氣訊號的量測，初步結果顯示東沙島東側測站的底質藻類覆蓋率及營養鹽高於環礁潟湖各測站；此外，整體的水氬訊號低，可能與當地地質環境有關，後續將於其他相近地質背景的島嶼環境進行測試。

中文關鍵字：東沙環礁，珊瑚島礁，地下水

英文關鍵字：Dongsha Atoll, Reef island, Submarine groundwater

Cold surge episodes in East Asian winter Monsoon (EAWM) and its effect on the boundary layer over the SCS

Chung-Hsiung Sui

Department of Atmospheric Sciences, National Taiwan University

This is a progress report of the project “Cloud, radiation, atmosphere-ocean boundary layer processes, and South China Sea (SCS) monsoon” (2020/12 to 2022/6). The objective of the project is to use atmosphere and ocean data observed/derived for SCSTIMX and models to study “atmosphere-ocean boundary layer processes” and “aerosol-cloud-precipitation-monsoon interactions”. Our ongoing analysis focus on the cold surge episodes in the winter (December and January) of 2020/2021 following the SCS Two Island Monsoon Experiment (SCSTIMX), and another five winters from 2006/07 to 2010/11 when Cloud Sat data is of best quality. The cold surge episodes are defined by three criteria: northerly wind in northern SCS ($V_m > 8 \text{ m s}^{-1}$); surface air temperature (T_S) at Kaohsiung/Hong Kong drops more than 4°C in 48 h & the lowest T_S falls to 14°C or lower; 6-day low-pass filtered northerly mass flux in the lower troposphere at (90-135E, 45N) is larger than one standard deviation.

The overall results indicate the boundary layer in northern SCS is convective with distinct inversion in response to the meridional overturning circulation of subsiding northeasterly EAWM from northern China-Korea and the southwesterly flow above the lower-troposphere monsoon flow. The upper air sounding data taken at Dongsha station in SCS shows the boundary layer consisting of mixed layer (mean depth 560 m and standard deviation 280 m) and convective PBL (mean depth 1610 m and standard deviation 600 m). The widely used assimilation data like the ERA5 does not resolve the inversion as clear as the sounding data show and tends to under-estimate the PBL height. Both sounding data and ERA5 data for strong cold surge episodes show the passage of a cold surge over northern SCS tends to cause a drier/colder PBL with a stronger subsidence and enhanced air-sea fluxes (due to enhanced wind speeds and larger air-sea temperature differences). Combining ERA5 and CloudSat and CALIPSO data for major cold surge episodes, we find the winter monsoon circulation in SCS is accompanied with stratocumulus in the PBL and cirrus clouds in upper-troposphere (10-16 km) that is originated from tropical convective system south of Taiping island (~10N). The convective-mixing processes in the PBL await to be analyzed next.

中文關鍵字：大氣海洋邊界層； 英文關鍵字：atmosphere-ocean boundary layer

東沙島與台灣間之海面大氣擾亂和電離層高頻通訊初步結果

Early Results of Sea-surface/atmospheric fluctuations and ionospheric HF communications between Dongsha Island and Taiwan

劉正彥(1,2,3)、陳耀淳(1)

(1) 1 國立中央大學太空科學與科技研究中心

(2) 國立中央大學太空科學與工程學系

(3) 國立中央大學太空與遙測研究中心

中央大學電波科學研究室二十年來即設置有五個頻段之電離層高頻都卜勒探測系統，持續例行觀察台灣地面上空之太陽閃焰、日食、颱風、地震所引起之移行電離層擾亂。本計畫正增建置收機於東沙島和太平島，用以接收來自台灣高頻都卜勒探測系統所發射之五個電波頻段，並藉此評估台灣與兩島間的海面波動、對流層擾亂、通訊環境之日、季、太陽活動變化。2021年7月8日已完成東沙島高頻都卜勒探測系統接收站之建置。初步結果顯示東沙島接收的都卜勒頻移與台灣本地的，於日夜變化有截然不同之現象。藉由電離層探測儀和福爾摩沙衛星七號觀測和模式比對，除可獲知高頻電波訊號於各個接收站之最佳使用頻段，並可一窺颱風電離層都卜勒移行擾亂傳播。未來將持續研究東沙島太平島與台灣間之間地震雷利波、海嘯、海波等引起之海面擾動，惡劣天氣、鋒面、颱風等所引發的對流層與移行電離層擾亂，以及高頻電波通訊品質。

中文關鍵字: 電離層、高頻、都卜勒、移行電離層擾亂

英文關鍵字: Ionosphere、high frequency、Doppler、traveling ionospheric disturbance

新南向國家利用衛星地球觀測及掩星資料在災防應用的技術輸出

劉小菁(1)、楊善國(2)

(1) 國家實驗研究院 國家太空中心地面研發處

(2) 國家實驗研究院 國家太空中心企推組

近年來自然災害對社會所造成的衝擊與時俱增，故遙測衛星任務對災防應用相關需求之重要性亦為人所日益重視。利用遙測影像可以快速評估諸如水災、地震、土石流或是其他災害所造成的嚴重性與損害衝擊。

本計畫輸出台灣經驗，推廣新南向國家利用衛星地球觀測及掩星資料在災防應用。協助南向諸國做農業監控，國土規劃、災害管理，維持國家安全與緊急救災支援的自主與即時性。

計畫類比企業行銷，無論透過推廣爭取商機或合作促進交流，一步一腳印，要在中日韓已深耕多年的地盤插旗，建立台灣的影響力。

主要目標：透過地球科學科研與知識研究加強與新南向國家合作關係，將我國研究強項與他國可能需求找出交集。推展雙向多邊多元合作，尋求突破，強化合作協議工作內涵和深化科技外交重大效益。目前已執行之成效如下：

- 連結在地國家級學研單位，建立資料立方，Open Data Cube (ODC) 的海外示範：泰國：重要經濟作物的蟲害監控；越南：土地崩塌(Land Slide) 監測。
- 辦理系列訓練課程或研討會，連結湄公河流域的國家的災防國家單位及研究機構，實務研討如何利用地球觀測及掩星資料的能量與技術來做災防(如淹水，森林大火)，及農業經濟等應用，進而建立合作計畫。
- 輸出台灣世界領先的掩星資料的應用，用於氣象，如颱風路徑，豪大雨預測；及用於太空天氣，大地震預警等。辦理 GNSS RO 研習營，總計 20 國 160 人與會，其中 8 國，106 人為新南向國家學員。

研發無人船(機)建構新南向國家的智慧海岸災防

呂政豪¹

¹國立澎湖科技大學觀光休閒系

東南亞的自然災害頻繁，其中最大的災害風險主要來自於極端海洋事件，有颱風和海嘯等災害，以及間接觸發的洪水溢淹、地滑和海岸侵蝕，再加上此區域的巨型大城市多位在海岸區，而氣候變遷將更加劇極端氣候的災害風險。故本計畫將聚焦於新南向國家的海洋極端事件的智慧災防，希望透過技術研發以及跨國的學術交流合作，得以協助東南亞區域國家在面對嚴峻的海洋災害事件時，能提出適當的調適及智慧防災作為。

截至首年的執行成果，本計畫已完成自製 PPK 高精度航測技術的研發與精度驗證，經實地驗證，在未佈設控制點下，自行研發的 PPK 無人機航測可達到公分級精度，此技術未來可移轉至新南向國家進行坡地與海岸監測，相關文章亦在準備中。在與新南向國家的合作上，子計劃主持人與河內太原大學的研究團隊建立夥伴關係，除共同討論研提雙邊合作計劃外，亦會將無人機航測技術轉移給太原大學運用於坡地監測上，規劃先採視訊教學或撰寫相關英文教學文件，待疫情解封後，再採實地教學。未來，本團隊將持續研發 MIT 的自製無人探測船，並將相關技術分享新南向國家之夥伴，深化本計畫之執行效益。

中文關鍵字:無人船、無人機、新南向計畫、智慧災防, 極端海洋事件

英文關鍵字:autonomous surface vehicle, unmanned aerial vehicle, new southbound program, smart disaster prevention, extreme marine event

Probabilistic seismic hazard assessments for Myanmar and Vietnam

Chung-Han Chan

Earthquake-Disaster & Risk Evaluation and Management (E-DREaM) Center, National Central University, Taiwan

Although Myanmar and Vietnam are earthquake-prone countries, neither of them has proposed an official national seismic hazard map. Thus, based on international collaborations, we conducted seismic hazard assessments for the two countries and some of their metropolitan areas.

Applying these assessments requires a set of databases that incorporates both earthquake catalogs and fault parameters. For Myanmar, we obtained seismic parameters from the International Seismological Centre, and we accessed a local catalog summarized by the Institute of Geophysics, Vietnam Academy of Science and Technology for the Vietnam region and its vicinity. The fault database includes fault parameters from paper reviews and the database summarized by the Taiwan Earthquake Model.

To evaluate the ground-shaking behaviours for Myanmar, we proposed a new set of ground motion prediction equations (GMPEs) based on the observations recorded by a broadband seismic network installed by the collaboration between the Earth Observatory of Singapore – Department of Meteorology and Hydrology – Myanmar Earthquake Committee and the Myanmar national broadband seismic network. In the case of Vietnam, we implemented the GMPE sets for various areas in Vietnam summarized by Le Minh Nguyen (personal communication).

By incorporating the V_s^{30} (the average shear velocity down to 30 m depth) map from analysis of topographic slope, we utilized site effect and assessed national probabilistic seismic hazards for the two countries. Additionally, we proposed detailed hazard assessments for some specific sites in several urban cities in the two countries, considering site conditions evaluated by microtremor measurements. The sites with low V_s^{30} or/and close to an active fault with a high slip rate obtain high hazard levels. The outcomes of this study will be beneficial to urban planning on a city scale and building code legislation on a national scale, and provide crucial information for Taiwanese businessmen and their investment plans.

The analysis of the 2020 Hpakant Jade Mine slope failure event using multi-sensor data integration

Yunung Nina Lin¹、Edward Park²、Yu Wang³、Yu-Pin Quek²、Jana Lim²、
Enner Alcantara⁴、Huuloc Ho⁵

(1)Institute of Earth Sciences, Academia Sinica, Taiwan、(2)National Institute of Education, Nanyang Technological University, Singapore、(3)Department of Geosciences, National Taiwan University、
(4)Department of Environmental Engineering, Sao Paulo State University, Brazil、(5)Water Engineering and Management, Asian Institute of Technology, Thailand

Northern Myanmar is currently the largest jade mining area around the world, with most of the mining activities occurring near the Hpakant area. The rapid expansion of jade mining in the past decade has significantly modified the topography, and triggered frequent fatal landslides in the mining quarries. The landslide in the Wai Khar open-pit jade mine on 2 July 2020 is one of the recent examples of quarry failure in the region, killing at least 172 jade miners in one single failure event. In order to understand the landscape evolution and the potential causes of this landslide, we integrate remote sensing observations from both optical satellite images and Sentinel-1 InSAR time-series, together with multi-temporal digital elevation models (SRTM and AW3D30), Landsat-based soil moisture time-series, CHIRPS precipitation time-series, and the video footages of the mining site before and after the landslide, to investigate the change of the Wai Khar open-pit mine between 2000 and 2020. Our result points out that the Wai Khar mining site is under aggressive mining cycles exacerbated by frequent, uncontrolled landslides. The tailings, which many have been turned into the residential areas north of the quarry pit, shows rapid subsidence especially near the rim of the pit. Rapid compaction of the tailings likely causes water expulsion and induces seepage failure. Since the precipitation record suggests below-average rainfall in the beginning of the 2020 monsoon season, the occurrence of landslide means the sliding planes were already in critical state. This critical state is manifested by the accelerated subsidence around the collapse area since the beginning of 2020. Altogether, our study suggests the Wai Khar open-pit failure is not directly caused by extreme rainfall, but by the combinations of weak geology and improper planning/management of the mining site.

Keywords: open-pit mine, slope failure, seepage failure, tailing subsidence, InSAR time-series, phase linking

利用東沙島珊瑚微型環礁重建南海近代海水面歷史

劉司捷¹、徐濤德¹、王昱¹、宋克義²

1. 國立臺灣大學地質科學系
2. 國立中山大學海洋科學系

全球海水面自工業革命以來持續地上升，已經成為海岸環境以及濱海都市的一大潛在威脅。當代海洋測高衛星的觀測顯示，全球海水面的上升在地理上分布其實並不均勻，常在特定海域有較高的上升速率。地處臺灣西南海域的南海即為一例，其海水面在數年之間的上升速率可以高達每年 1 到 2 公分，倘若該地區海水面的長期上升趨勢與此觀察相符，則南海周邊海岸，包括周邊多個國家的許多濱海大城市，將會在近期面臨海面上升的相關災害。東沙島座落於南海海盆北緣，且遠離周圍陸地，因此是一探討南海海面上升過程的理想地點。

珊瑚由於其最高生存面高度大致受到海水面低潮線的限制，一旦珊瑚群體高度與其最高生存面達成平衡，可形成所謂的微型環礁，此一特殊外型與其生長紋可以記錄年解析度的相對海水面歷史。本研究於東沙島北岸進行調查，並採集前人報導的現生珊瑚微型環礁族群，藉以重建南海近半世紀以來的相對海水面歷史，初步結果顯示東沙島附近的海水面平均上升速率約為每年 4 公釐左右。後續將繼續針對採得的珊瑚微型環礁群體樣本進行分析，希望能夠建立南海海盆北部工業革命以來的詳盡海水面變化歷史，對未來該地區海岸環境相關災害將有很大助益。

Scenario tsunami triggered by submarine landslide at northern offshore of Sumatra island and its hazard Assessment

Haekal A. Haridhi^{1,9,10}, Bor Shouh Huang², Kuo Liang Wen³, Arif Mirza⁴, Syamsul Rizal¹, Syahrul Purnawan¹, Ilham Fajri¹, Frauke Klingelhoefer⁵, Char Shine Liu⁴, Chao Shing Lee⁶, Crispen R. Wilson⁷, Tso-Ren Wu⁸, Ichsan Setiawan^{1,9,11} and Van Bang Phung²

¹Department of Marine Sciences, Faculty of Marine and Fisheries, Universitas Syiah Kuala, Banda Aceh, Indonesia.

²Institute of Earth Science, Academia Sinica

³Department of Earth Sciences, National Central University

⁴Institute of Oceanography, National Taiwan University

⁵Ifremer, Department of Marine Geoscience, Plouzané, France.

⁶Institute of Geosciences, National Taiwan Ocean University

⁷Asian Development Bank, Mandaluyong City, Philippines.

⁸Graduate Institute of Hydrological and Oceanic Sciences, National Central University

⁹Research Center for Marine Sciences and Fisheries, Universitas Syiah Kuala, Banda Aceh, Indonesia.

¹⁰Tsunami and Disaster Mitigation Research Center, Universitas Syiah Kuala, Banda Aceh, Indonesia.

¹¹Graduate School of Mathematics and Applied Sciences, Universitas Syiah Kuala, Banda Aceh, Indonesia.

Near the northern end of the Sumatra island, the right-lateral strike-slip Sumatra Fault Zone split to two branches and vanished after its coast. This fault zone has been traced to continuously extend to offshore by seismic sounding surveys. However, due to its strike-slip faulting characteristics, the activity of the Sumatra Fault Zone is rarely considered for tsunami hazard issues in this region. Based on two reprocessed reflection seismic profiles, the image shows that the extended Sumatra Fault Zone strongly related to some chaotic facies indicating evidence of large triggered submarine landslide ever occurred. According to the recently acquired high-resolution shallow bathymetry data, some coastal steep slopes and new subsurface characteristics of submarine landslide depose were mapped. Four shear faults were identified in conjunction to the slip movement of the main fault system beneath the low altitude plain and its shallow coast region. Based on the slope stability analysis, it indicates that some targets with steep morphology are close to failure. Tsunami scenarios were considered as a combined effect of earthquake and its triggered submarine landslide at those target sites. In extreme case, an earthquake with magnitude Mw 7 or larger occurred and its strong ground shaking triggered a submarine landslide at northern offshore of Sumatra island.

The induced water perturbation may generate a tsunami hitting the coast. Based on a simulation of tsunami wave propagation in shallow water, the wave highs can be near 4 meters at some locations of coast. Conclusion of this study indicate the potential tsunami hazard from the submarine landslide triggered by a strike-slip fault system. The further landslide tsunami hazard assessment and early warning system in this study area can be learn from this proposed scenario.



Characteristics of earthquake source and ground motions in northern Vietnam investigated by the 2020 Moc Chau M5.0 earthquake sequence

Nguyen Cong Nghia¹、Van Duong Nguyen²、Le Minh Nguyen³、
Van Bang Phung⁴、Bor-Shouh Huang⁴、Anh Duong Nguyen³、
Quang Khoi Le³、Thi Giang Ha³、Dinh Quoc Van³、Ha Vinh Long⁵

(1)Taiwan International Graduate Program Earth Sciences System, Academia Sinica, Taiwan、

(2)Institute of Geophysics, Vietnam Academy of Science and Technology, Vietnam; Graduate University of Science and Technology (GUST), Vietnam Academy of Science and Technology、

(3)Institute of Geophysics, Vietnam Academy of Science and Technology, Vietnam、(4)Institute of Earth Sciences, Academia Sinica, Taiwan、(5)Taiwan International Graduate Program Earth Sciences System (TIGP-ESS), Academia Sinica, Taiwan; Institute of Geophysics, Vietnam Academy of Science and Technology, Vietnam

On July 27th, 2020, a magnitude (M_w) 5.0 shallow earthquake occurred near Moc Chau, northwestern Vietnam. Several shallow aftershocks followed the mainshock and clustered in a small area. The mainshock caused damage to infrastructures in the source area. Significant shakings were felt at many new high buildings in surrounding cities. The ground motions of the mainshock and its aftershocks were well recorded by the national seismic network of Vietnam to analyze this earthquake sequence. The focal mechanisms of these events showed their major contribution from strike-slip movements. After this earthquake, a field survey has been carried by the research team of the Institute of Geophysics, Vietnam Academy of Science and Technology, Vietnam. A combination of damages pattern and source mechanism from moment tensor inversion analysis reveals this earthquake sequence might be associated with the active right-lateral Da River fault. The new archived seismic observations of this earthquake sequence have been analyzed to evaluate characteristics of earthquake source and seismic wave propagation in northwestern Vietnam and to discuss its potential earthquake engineering applications in northwestern Vietnam.

Keywords: Moc Chau earthquake, focal mechanisms, strike-slip fault, ground motion

Source investigation for earthquakes along Flores Thrust, Indonesia

Dimas Sianipar¹、Bor-Shouh Huang²、Kuo-Fong Ma³

(1)Taiwan International Graduate Program (TIGP) Earth System Sciences, Academia Sinica and National Central University; Agency for Meteorology, Climatology, and Geophysics of the Republic of Indonesia (BMKG), Jakarta, Indonesia、(2)Institute of Earth Sciences, Academia Sinica, Taiwan、(3)Institute of Earth Sciences, Academia Sinica, Taiwan; Earthquake-Disaster and Risk Evaluation and Management Center (E-DREaM), National Central University

The south-dipping, low-angle Flores Thrust in Indonesia hosted damaging $M_w > 6$ earthquakes, including the 1992 M_w 7.7 Flores earthquake-tsunami and most recent the 2018 Lombok earthquake sequence that claimed more than 500 casualties and resulted in severe damages. However, the characteristics of the earthquake ruptures and their relations to regional tectonic were poorly investigated. Here we study the source time functions and possible rupture models of ten M_w 6.2+ earthquakes along Flores Thrust through finite fault inversions. Our inversions were constrained with the teleseismic body- and surface-waves and the updated information of the seismicity from both global and Indonesia regional seismic networks. The model uncertainties were computed by performing statistical jackknife tests. We find that cascading asperities ruptured neighbor fault patches in western Flores Thrust, including the 2002-2009 Sumbawa sequence (5 events) and 2018 Lombok sequence (3 events). The ruptures were often initiated from the mid-crust and propagated unilaterally. We discuss the idea that this cascading feature of moderate magnitudes (M_w 6-7) might be related to fault immaturity. The cluster of M_w 6-7 cascading earthquakes implies that the western Flores fault prohibited the growth of a single large earthquake ($M_w > 7$). We further discuss the rupture characters of the fault (e.g., initiation, the rupture speed, stress drop) by comparing the western and eastern Flores Thrust. The nature of shallow rupture of M_w 6-7 beneath the northern coast of island arcs favors the high seismic and tsunami hazard to the region. Thus, this study is essential to provide the rupture characteristics and asperity locations along the Flores Thrust necessary to evaluate the region's earthquake and tsunami hazard.

Keywords: asperities, finite-fault, Flores Thrust, rupture, source-time-functions

地質保育發展史—科學、襲產、到整全的生態人文保育

紀權宵¹

(1)地創地質顧問有限公司、臺灣師範大學地理學系

地質保育(geoconservation)一詞在 1990 年代才被提出，其定義為保育地球的特徵與系統的多樣性，然而地質保育的概念在 19 世紀的英國已經開始萌芽，從具有特殊科學價值的地質景點或露頭開始產生保育的意識。日本 1919 年以及英國在 1949 年已制定法案針對其國內具有科學價值的地質與地形景點進行調查與保護，1970 年代起，澳洲與歐洲興起地質科學保育的風潮，1994 年由 IUGS 推動 Geosites 計畫使此風潮在達到最高峰，我國也這個時期推動全國的特殊地質與地形景觀普查。地質遺產保護的國際倡議始於 1972 年的《世界遺產公約》，同年我國也頒布《國家公園法》來保護珍貴的地質、地形自然遺產。1982 年《文化資產保存法》以自然保留區來保護特殊地形與地質的現象，至 2016 年二度修法，並增列自然紀念物(特殊稀有礦物、特殊地質地形現象)與地質公園等類別。1991 年歐洲地質遺跡保育協會發布「守護地球記憶權利宣言」，讓地質保育與全球的環境及社會議題開始對話，進而促成「地質多樣性(geodiversity)」概念的興起，以及 1997 年 UNESCO 推動世界地質公園計畫，將地質科學的重要性，連結到生態、文化與經濟的永續發展議題。國內雖已將地質保育的概念納入各項法規中，但仍缺乏地質科學為主軸的實務作為，地質僅被視為生態保育、觀光旅遊中的一個項目。30 年來國際地質學者努力開啟跨領域以及與社會的對話，如今國內的地質科學界應該一同思考如何突破國內的困境。

中文關鍵字：地質保育、地質遺跡、地質公園、地質多樣性、文化資產保存法

網路社群在地質知識推廣及民情反映之應用

王豐仁¹、林建緯²、郭麗秋³、侯進雄³

(1)臺灣省應用地質技師公會、勝田工程技術顧問有限公司、(2)臺灣省應用地質技師公會、
(3)經濟部中央地質調查所

網路社群是現今資訊時代生活中重要的一環。它是溝通的方式，也是社交的平台，更是推播教育的工具。經濟部中央地質調查所辦理之「地質知識網絡推動發展計畫」中，自 101 年開始利用臉書(Face Book)設立「地質知識網絡」臉書社群，由此作為傳遞地質知識、宣導地質觀念、協助推動地質法規、激發國人對於地質環境的認知。

而經由網路社群貼文地質知識議題的規劃，或圖文屬性的操作，可以發現對於讀者的點擊率、按讚數、留言回應數等，都有不同的效果，藉此，可以蒐集分析民眾對於不同地質議題或是地質法規的關注度差異，以及反應的強度。同時，經由民眾所屬地理位置的分析，可以進一步分析了解不同地區民眾對於該地質議題的關注度、或是對於該議題的民情反應趨勢，藉此，一方面將有助於地質知識的推廣，一方面亦有助於地質法規的意見蒐集與推動。

中文關鍵字：地質網路社群、傳遞地質知識



「創意地質旅遊」興起的社會參與及實用價值

郭麗秋¹、陳政恒¹、董英宏¹、黃芷馨¹、侯進雄¹

(1)經濟部中央地質調查所

地質旅遊(geotourism, tourism geology)，也稱作地景旅遊、地學旅遊等，是經常被用以探討地質資源利用的選項之一，在 Hose 於 1995 年提出地質和地貌可從審美的角度提供服務或設施而成為旅遊後，漸於全球發展。地質旅遊以地質為主角，搭配科學、文化、教育、價值、景觀、美觀、娛樂、威脅或風險、經濟、自然保護、管理等面向，帶入地方可提升旅遊品質、社區意識與特色環境的突顯；成為教學課程則能加深學生對地球起源、人類文化與環境現狀的洞察；對整體環境而言，有利於地質遺跡保育及地質災害事件借鏡。聯合國教科文組織(UNESCO)推動地質公園，地質旅遊便與地景保育、社區參與及環境教育等功能，並列四大核心價值。

臺灣「創意地質旅遊」一詞首先出現在 2012 年 9 月《地質》季刊，當時是地質法與環境教育法上路的第二年，推廣地質教育受到鼓舞正方興未艾，於是乎《地質》編輯委員會熱烈討論，想要催生給地科老師參考用的地質考察路線，也希望為民眾推薦輕鬆可及的地質知性旅遊景點。「創意」是時尚口號，激發編輯人員以「創意」套用在「地質旅遊」，規劃「北北基創意地質旅遊」12 條路線專題，並向地質從業喊話邀稿，最後由 11 位作者在被設定的段落、字數、順遊資訊、簡單文字、生動圖片等規格下寫作，呈現每 1 路線的地質景點及附近的名產或名勝等。北北基 12 條路線在《地質》專題被發行後，陸續搭配新聞稿及記者會露出，引發不少媒體報導；後於國際書展、旅展或機場展等場合，請作者在「地質小學堂」舞台上親口向民眾解說，既專業又知性的安排顯得新鮮有趣，而吸引眾多民眾駐足聆聽；如此一連串的行銷也獲得地質與環境領域人士的關注與討論。「創意地質旅遊」從此順利發酵，至 2020 年時，已經依序出版中彰投 6 條、花東 10 條、恆春半島 7 條、高屏 9 條、雲嘉南 11 條、桃竹苗 10 條，未來加上離島地區，全國將會有至少百條地質賞析路線被推薦一遊。

「創意地質旅遊」可以說是傳統的地質圖、文資料重新包裝上市的地質產品，其實並未被局限於以此為名而規劃的地質路線，其他因地質遺跡地質敏感區、地質公園、步道地質、公路地質等主題而推薦的地區或景點，都是在表現臺灣原創的山、川、土、石、火、海、島之多樣性，均可以是創意地質旅遊之處。這些地質旅遊路線的圖文在著作授權後，跟著被導入到地質推廣的各個工作上，例如地質知識漂、地方特色地質輔導、地質主題網站、社群臉書貼文等，成為重要的教材與資料源，相當程度幫助了地質科學擴大社會參與並提升實用價值。

可惜因為成本投入有限，各分區的地質旅遊路線多在短時間內出版，可能有遺珠之憾；也還未形成足夠的影響力，讓更多生態、旅行、交通、路跑、健康或媒體等等業者，瞭解到其活動或報導所倚賴的山光水色根源於地質演化，因而漏

失不少異業連結、彼此互補的機會。這些美中不足之處，卻鋪陳了「創意地質旅遊」精進的藍圖，未來可透過盤點方式增修地質路線與周圍的生活資訊，再次包裝上市，加速降低各行各業與社會大眾普遍不認識地質環境之情況。

中文關鍵字：創意地質旅遊、地質產品、地質推廣、環境教育



東海岸寬闊河口區的河階地發育模式

陳佳宏¹、吳庭瑜²、齊士崢¹、顏君毅³

(1)高雄師範大學地理學系、(2)經濟部中央地質調查所、(3)東華大學自然資源與環境學系

在上個世紀中期，地形學者使用一個罕見名詞「thalassostatic terraces」，說明從 glacial minimum 到 interglacial climatic optimum 這段期間，因海水面快速上升，導致海岸地帶和流域下游被上漲的海水淹沒(或上漲海水面影響)而加積，由堆積作用形成寬闊的平原或河谷平原(對應於由侵蝕作用形成的準平原(peneplain))；然後從 interglacial climatic optimum 到 glacial minimum 期間，海水面下降，河川自堆積形成的平原面下切，殘餘的堆積平原面形成河階地。根據國家教育研究院雙語詞彙、學術名詞暨辭書資訊網將「thalassostatic terraces」翻譯為「海升期河階」，然所有河階地都生成於廣義的侵蝕基準面下降期，這樣的翻譯應該不易讓人理解這類型階地發育的含義；故猜測「海升期河階」的譯名原因應是強調階地面這個「平面」是海升期堆積或河谷埋積形成的。我們在港口溪、金崙溪、馬武窟溪、豐濱溪和水璉溪等等流域的研究中，發現在近河口區經常出現階地崖出露厚層沉積層的階地，部分階地崖底部以下可能還有厚層的沉積層，且這套沉積層的堆積開始時間大約就在末次冰河時期結束之後到全新世氣候最適宜期，或全新世高海水面時期，有一個明顯可以和「下切期」區隔的「堆積期」，或有「老的沉積物」和「年輕的階地面」。因此，這些階地似乎都是「thalassostatic terraces」，但階地沉積層的堆積開始時間與結束時間並不十分吻合於 glacial minimum 和 interglacial climatic optimum 時間點，或它們的發育並不完全反映海水面變化過程，所以這些階地並非典型的「thalassostatic terraces」。我們認為在台灣不容易出現典型的「thalassostatic terraces」的影響因素，包括地形發育過程中持續的海岸線位置變化、陸地抬升速率和河川供應沉積物特徵的種種差異。

中文關鍵字：海升期河階、河階地、冰期最小期、間冰期氣候最適宜期

Identification and discrimination of two invasive cryptic species and development of methodology for environmental DNA (eDNA) barcoding

Pritam Banerjee¹、Gobinda Dey²、Raju Kumar Sharma³、
Caterina M. Antognazza⁴、Himani Kumari⁵、Michael W.Y. Chan⁵、
Jyoti Prakash Maity⁶、Chien-Yen Chen⁶

(1)Department of Earth and Environmental Sciences, National Chung Cheng University; Department of Biomedical Science; Graduate Institute of Molecular Biology, National Chung Cheng University、

(2)Department of Earth and Environmental Sciences, National Chung Cheng University; Department of Biomedical Science, Graduate Institute of Molecular Biology, National Chung Cheng University、

(3)Department of Chemistry and Biochemistry, National Chung Cheng University; Department of Chemistry and Biochemistry, National Chung-Cheng University、(4)Department of theoretical and

applied science, University of Insubria, Varese, Italy、(5)Department of Biomedical Science, Graduate Institute of Molecular Biology, National Chung Cheng University、(6)Department of Earth and

Environmental Sciences, National Chung-Cheng University

Golden apple snails (*Pomacea* spp.) are the freshwater gastropod, were introduced during the 1980s in East and South-East Asia, are considered the top hundred destructive introduced species in the world. They are marked as a serious concern due to the destruction of agriculture by its excessive growth and overconsumption of plants (e.g. reduced rice production), spreading of life-threatening diseases by carrying pathogens, (e.g. intermediate host of *Angiostrongylus cantonensis*), and outcompeting native populations. However, few beneficial roles in food and fodder due to high protein content in tissue, use of the shell in production of cement, fertilizer, catalyst/ reagent of heavy metal removal, drug delivery, bone grafts, biofuel production, suggesting the potential utilization. Although, the lack of clear taxonomy and proper detection method affecting the control of invasiveness. Besides, misidentification can mislead researchers during application. Considering this background, present work focusses on the identification and discrimination of two cryptic invasive species, *Pomacea caniculata* and *P. maculata* from shell structure to molecular genetic level to maintain a clear taxonomy and emphasize on development of a standard protocol for detection of eDNA from both *Pomacea caniculata* and *P. maculata* in a mesocosm. Our study shows that in spite of failure in detection of those two species morphologically, a molecular level detection and monitoring can be used to detect species non-invasively. Nevertheless, as we found some minor differences in snail shell properties and structure, a strong need to distinguish species is obligatory. Furthermore, the development and validation of eDNA method for cryptic invasive species will be highly effective to survey the hidden biodiversity in the introduced places.

Keywords: environmental DNA, cryptic species, golden apple snail, molecular taxonomy, biodiversity monitoring



Methane rare isotopologue signals associated with methanotrophy in freshwater reservoir

Yeah-Ting Lin¹、Jhen-Nien Chen¹、Pei-Ling Wang²、Edward D. Young³、
Tzu-Hsuan Tu⁴、Li-Hung Lin¹

(1)Department of Geosciences, National Taiwan University、(2)Institute of Oceanography, National Taiwan University、(3)Department of Earth, Planetary and Space Sciences, University of California Los Angeles, USA、(4)Department of Oceanography, National Sun Yat-sen University

Methanotrophy plays an effective role in reducing the export of greenhouse methane from subsurface environments to the atmosphere over geological and contemporary time scales. In sediments or bottom water of freshwater lake, sulfate and oxygen are often scarce, thereby facilitating anaerobic methane oxidation potentially coupled to various electron acceptors. Quantifying the rates, pathways and regulatory factors of methanotrophy remains challenging as unique isotopic signatures associated with methane producing and consuming metabolisms are obscured by transport and mixing. Paired rare isotopologues of methane provide two dimensions in addition to bulk isotopes to describe isotopic re-equilibration and kinetics. In this study, we measured the abundances of rare methane isotopologues and companion characteristics derived from anaerobic incubation of sediments collected from the Feicui reservoir. Bulk isotope values of residue methane increased through time, generating fractionation factors of 1.01 for carbon and 1.07 for hydrogen. The $\Delta^{13}\text{CH}_3\text{D}$ and $\Delta^{12}\text{CH}_2\text{D}_2$ values were distributed in the proximity of the equilibrium line toward the high temperature end, a range greatly exceeding the incubation temperature (by hundreds of Celsius). Overall, the apparent equilibrium pattern suggests the unique kinetic control on the re-organization of rare isotopes in methane isotopologues during methanotrophy. Further deconvolution of mass balance is warranted.

Keywords: clumped isotopologues, methanotrophy, freshwater environments

菲律賓全新世珊瑚礁之微生物化

徐鈺婷¹、湯森林²、張英如¹、宮守業³

(1)臺灣海洋大學地球科學研究所、(2)中央研究院生物多樣性研究中心、(3)國立自然科學博物館

微生物岩(Microbolite)是由於底棲微生物群落在進行生理活動時，將碎屑沉積物凝聚、進行礦物沉澱或生物礦化等作用而產生生物沉積岩。菲律賓 Pararior 海岸之全新世(Holocene)岩芯中發現珊瑚礁與微生物岩交疊生長的狀況，而新生代珊瑚礁與微生物各指示著不同的環境條件，因此，其共生長的案例相當稀少，具有研究上的獨特性。Pararior 海岸珊瑚礁岩芯透過光學顯微鏡發現珊瑚礁最先被紅藻、有孔蟲覆蓋，接著是微生物岩生長，本研究試圖利用分析珊瑚、藻類及微生物岩之微生物群落，佐證藻類的存在可能改變珊瑚的生長狀態及其微生物菌相，進而促使微生物岩的生長。本研究萃取珊瑚礁岩芯之 DNA，進行 16s RNA 次世代定序，建立微生物群落庫。結果顯示岩芯 PAR 5 深度 15 與 15.1 公尺兩處微生物岩之微生物群落單元相似度為 97%，大多為兼性厭氧與厭氧菌。平均組成為 98.5%細菌(Bacteria)以及 1.42%古菌(Archaea)。細菌中占比最高為擬桿菌科(*Bacteroidaceae*)占 21.2%與理研菌科(*Rikenellaceae*)占 12.5%，分析結果多為厭氧與兼性厭氧之異營菌，而異營菌的生長及碳酸鹽沉澱會隨著有機質而遞增。珊瑚表面之肉質藻類與草皮藻類會釋放容易被微生物利用之溶解有機碳(Dissolved Organic Carbon, DOC)，促進對珊瑚有害之異營微生物生長，直接造成珊瑚微生物群落之改變。根據 Christophe Dupraz 和 Andre Strasser 所建立之珊瑚轉為微生物相之沉積環境，推論本研究可能處於低濁度營養相過度為高營養相之環境，以至於有利於微生物岩生長。本研究將繼續萃取岩芯中同深度之珊瑚、藻類、微生物岩與沈積物之 DNA，探討不同介質上之微生物菌相的轉變以及所代表的環境意義，建構珊瑚、藻類、微生物三者間之生長模式。

中文關鍵字：微生物岩、珊瑚礁、藻類、微生物化、次世代定序、全新世

The biofuel production by indigenous algae along with wastewater treatment

Pulipaka Naga Venkata Anoohya¹、Pritam Banerjee²、Gobinda Dey²、
Raju Kumar Sharma³、Jyoti Prakash Maity¹、Chien-Yen Chen¹

(1)Department of Earth and Environmental Sciences, National Chung-Cheng University、
(2)Department of Earth and Environmental Sciences, National Chung Cheng University; Department of
Biomedical Sciences, National Chung Cheng University、(3)Department of Chemistry and
Biochemistry, National Chung-Cheng University

Enormous consumption of fossil fuels is unsustainable as a consequence of depletion of global reserves and increasing concerns about its contribution to global warming. Microalgae represent a viable alternative energy resource, which can produce large volumes of biomass, and subsequently biofuels, in much smaller geographic areas than first- and second-generation biofuels production. This study describes algal biofuel production, wastewater treatment using indigenous algae. Moreover, along with the production of biofuel, the study focuses on to optimization of biomass production (algal cultivation and operation under optimal conditions, biomass harvesting and lipid extraction) with different wastewaters using indigenous algae (*Chlorella sorokiniana*, *Scenedesmus*). Furthermore, the investigation focusses on the pollutant removal from wastewater. Result reflects that the production of biofuel was increased with the incubation time and biomass production. The pollutant concentrations in wastewater were decreased with the increasing time in presences of green algae and biomass concentration. Interestingly, the biofuel productions with wastewater treatment are the best mitigation option of replacing fossil fuels, safe wastewater disposal, carbon dioxide mitigation, and heavy metal removal.

Keywords: renewable energy, indigenous algae, biofuel, wastewater treatment, heavy metal removal

Isolation and characterization of indigenous rhizospheric salt tolerant phosphate solubilizing bacteria from Puzi Mouth Wetland in Taiwan

Gobinda Dey¹、Pritam Banarjee¹、Raju Kumar Sharma²、
Jyoti Prakash Maity³、Hsien-Bin Huang⁴、Chien-Yen Chen³

(1)Department of Biomedical Science, National Chung Cheng University; Department of Biomedical Science, Graduate Institute of Molecular Biology, National Chung-Cheng University、(2)Department of Chemistry and Biochemistry, National Chung Cheng University; Department of Chemistry and Biochemistry, National Chung-Cheng University、(3)Department of Earth and Environmental Sciences, National Chung-Cheng University、(4)Department of Biomedical Science and Graduate Institute of Molecular Biology, National Chung Cheng University

Soil salinity is one of the major abiotic stress all over the world due to the reduction of cultivated agricultural land and crop productivity compared to the growing population. In addition, last 50 years, due to fulfill our food demand the excessive use of chemical fertilizer, pesticides like fungicides, herbicides that make environmental problems including groundwater contamination, soil quality degradation, heavy metal contamination, biodiversity reduction, and increasing salinity of the soil. To counteract the adverse effects of salinity and chemical fertilizer on plants and soil, the use of salt-tolerant phosphate solubilizing bacteria (PSB) is an efficient and sustainable method in saline agriculture practice. Considering the background, In the present investigation, we have searched for efficient salt-tolerant phosphate solubilizing bacteria, which were isolated from the rhizosphere of *Avicennia* sp. and *Rhizophora* sp. of Puzi mouth wetland in Taiwan, a typical saline land. A total six isolates of PSB strains are identified by using of 16S rRNA gene and comparative analysis confirmed the taxonomic affiliation of PSB1, PSB2, PSB3, PSB4, PSB5, and PSB6 with *Bacillus velezensis* strain GD CCU TW1, *Enterobacter coloaecae* strain GD CCU TW2, *Bacillus licheniformis* strain GD CCU TW3, *Bacillus* sp. strain GD CCU TW4, *Kocuria arsenatis* strain GD CCU TW5 and *Bacillus* sp. strain GD CCU TW6 respectively. All PSB has a high potential for dissolving calcium phosphate $[Ca_3(PO_4)_2]$ within the range of 55.20-119.03 mg/L and showed phosphate solubilizing index from 2.21 to 2.88, but relatively weak ability to dissolve $AlPO_4$ and $FePO_4$ under salinity. Moreover, all the strains are produced IAA with ranges from 1.20 to 24.07 mg/L and well grown under Arsenite (AsIII) in 5 Mm concentration. This study characterized salt-tolerant PSB isolates can be used as bio inoculants that may be applied in saline agriculture and arsenic bioremediation practice.

Keywords: salt tolerant, phosphate solubilizing bacteria, IAA, arsenite, sustainable

agriculture, bioremediation



A novel Bio-MCM-41 material: Synthesis using bacteria mediated biosurfactant and their characterization

Raju Kuma Sharma¹、Gobinda Dey²、Pritam Banerjee²、
Jyoti Prakash Maity³、Chien-Yen Chen³

(1)Department of Chemistry and Biochemistry, National Chung-Cheng University、(2)Department of Biomedical Science, Graduate Institute of Molecular Biology, National Chung Cheng University、
(3)Department of Earth and Environmental Sciences, National Chung-Cheng University

The mesoporous material synthesis has received a great attention in the field of material science due to their potential utilization as adsorbents, controlled drug delivery systems, sensors, catalyst in chemical reactions, acidic character, and cosmetics, etc. The different kinds of organic surfactants (e.g. CTAB, P123, F127, and CTAC, etc.) played an important role to synthesize the mesoporous material, where the material was introduced as less favorable in green nanotechnology due to their toxic effect. In the present study, a novel material Bio-MCM-41 was synthesized using a biological template as *Bacillus subtilis* BBK006 derived biosurfactant along with suitable precursor tetraethyl orthosilicate, which is a key objective to improve the green approach in nano-biotechnology. The material was prepared at room temperature with optimum pH and less time-consuming via sol-gel method. The key influence of synthesized material was studied at different calcinated temperatures such as 450 °C, 500 °C, 550 °C, and 600 °C respectively. The amorphous mesoporous silica characteristic was distinguished using low angle-XRD at d100, d110, d200 and wide angle-XRD at 22.59 (d100). The functional groups of calcinated material was observed at 3445 cm⁻¹ (-OH group), 802 cm⁻¹ (Si-O-Si). The FESEM and HRTEM micrograph of synthesized particle reflects the uniform spherical shape and specific particle diameter range of 250-300 nm. The TG-DTA result exhibits the removal of adsorbed surface water (30-210 °C), interlayered water molecules (210-307 °C), biological compound (307-468 °C), and formation of mesoporous silica nanoparticles (468-800 °C). The synthesized particles instituted a high surface area of 8.2616 m²/g and pore diameter of 14.8516 nm at calcinated temperature 550 °C. Thus, an eco-friendly novel material was synthesized using *Bacillus subtilis* and it can be applicable to the catalytic and environment research sector.

Keywords: mesoporous material, *Bacillus subtilis*, Bio-MCM-41, eco-friendly

台北都會區大氣中細懸浮微粒化學組成成分

林家恩¹、潘詩諭¹、練建國¹、紀凱獻¹、蕭大智²

(1)陽明交通大學環境與職業衛生研究所、(2)臺灣大學環境工程研究所

台灣將近七成人口居住於城市大都會區，而當人口密度提高時，人類活動所產生的污染排放量越多，比如在固定污染來源的空氣染物排放、因為車輛所造成的尾氣污染物以及其他可能影響空氣品質的沙塵暴事件等。而在空氣中的PM2.5為目前當今較被大眾關注的污染物，其本身附著在微粒上的化學成分會對人體健康產生危害如：多環芳香烴(PAHs)具有致畸性和致癌性以及金屬(trace metal)易造成神經和免疫系統的破壞等。本研究於台北都會測站進行實驗，分析大氣中PM2.5濃度以及化學成分，並探討日夜間及平假日變化外，同時也考慮事件日(境外長程傳輸LRT以及本土污染LP)及無事件日(normal)的發生；並進一步使用正矩陣因子法(Positive Matrix Factor, PMF)解析其污染物來源，最後以吸入性終生致癌增量風險(ILCR)來評估台北都會測站大氣中PM2.5所造成之健康風險。

研究結果顯示：都會測站於日夜間PM2.5濃度分別為 12.9 ± 5.64 ($\mu\text{g}/\text{m}^3$)和 10.4 ± 5.16 ($\mu\text{g}/\text{m}^3$)；而平假日的PM2.5日平均濃度則分別為 12.2 ± 4.96 ($\mu\text{g}/\text{m}^3$)、 10.3 ± 3.47 ($\mu\text{g}/\text{m}^3$)。比較有無事件日發生時，在non-event時PM2.5日平均濃度為 9.70 ± 3.62 ($\mu\text{g}/\text{m}^3$)，而當在event發生時，LRT的PM2.5濃度為 15.6 ± 5.45 ($\mu\text{g}/\text{m}^3$)、LP則為 21.7 ± 4.48 ($\mu\text{g}/\text{m}^3$)。而PAHs濃度在日夜間分別為 4.96 ± 6.48 ($\text{ng BaPeq}/\text{m}^3$)和 4.02 ± 7.89 ($\text{ng BaPeq}/\text{m}^3$)；平假日則為 2.89 ± 2.36 ($\text{ng BaPeq}/\text{m}^3$)和 3.27 ± 1.84 ($\text{ng BaPeq}/\text{m}^3$)；非事件濃度為 3.02 ± 2.50 ($\text{ng BaPeq}/\text{m}^3$)、LRT為 2.51 ± 0.293 ($\text{ng BaPeq}/\text{m}^3$)以及LP為 3.53 ($\text{ng BaPeq}/\text{m}^3$)，且在PAHs的物種分布中，不管是日夜間、平假日還是有無事件日發生都以高環數占比最高，特別是當LP發生時高環數占比又再增多，其主要與存在高環數物種的BghiP濃度較高有關。最後在水溶性陰陽離子之分布，不管在日夜間、平日假日還是有無事件日發生，主要離子皆包含 SO_4^{2-} 、 NH_4^+ 、 NO_3^- ；金屬元素之分布則都以Na、Fe、K為主。使用PMF進行解析本研究之都會測站大氣污染來源，解析結果得出3種主要污染貢獻來源，分別為交通車輛之汽油引擎(73.7%)、交通車輛之柴油引擎(12.2%)、燃煤電廠(12.2%)。最後暴露於都會測站PAHs之吸入性終生致癌增量風險(ILCR)之評估結果為日間($1.69 \pm 9.73 \times 10^{-5}$)、夜間($1.35 \pm 1.11 \times 10^{-5}$)；平日($1.66 \pm 6.63 \times 10^{-5}$)、假日($1.41 \pm 1.17 \times 10^{-5}$)；而在不同情境下normal($1.46 \pm 8.38 \times 10^{-5}$)、LRT($1.47 \pm 2.67 \times 10^{-5}$)、LP(2.60×10^{-5})，其暴露風險皆介於可容忍之限值($10^{-6} \sim 10^{-4}$)。

中文關鍵字：細懸浮微粒、多環芳香烴、痕量金屬、健康風險

PM_{2.5} and hazardous air pollutants: characteristics, source apportionments, and their health impacts

Ngo-Tuan Hung¹、Wei-Ting Hsu²、Yu-Hsuan Yang¹、Yina Lee¹、
Pei-Chun Tsai¹、Wen-Chi Pan¹、Kai-Hsien Chi¹

(1)Institute of Occupational and Environmental Health Sciences, National Yang-Ming Chiao-Tung University、(2)Institute of Occupational and Environmental Health Sciences, National Yang-Ming Chiao-Tung University; International Health Program, National Yang-Ming Chiao-Tung University

Different sources of air pollution can affect the composition of PM_{2.5} which in turn differently influence human health. In this research, we aim to study the sources of ambient PM_{2.5} in Taiwan and how they affect the human health. We focused on PCDD/Fs composition of PM_{2.5} for source apportionment analysis.

Air pollution was collected using high volume instrument at different places including industrial, urban, LRT, cooking areas. PM_{2.5} samples then underwent extraction and purification processes to obtain and separate different compositions. Organic compounds (PAHs, PCDD/Fs) were analyzed using GSMS, metal elements were quantified using ICP-MS, and ion chromatograph (IC) was employed to study ion composition. Source apportionment was done using PCA, PMF, and Bivariate Polar Plot coupling with cluster analysis. We conducted cytotoxic research for different sources of PM_{2.5} on cell model and epidemiological research to study association between concentration of PM_{2.5} from different sources and mortality.

PM_{2.5} and PCDD/Fs were highly correlated. Major sources of PM_{2.5} and PCDD/Fs in Taiwan were industrial activities, traffic activities, and also LRT (North of Taiwan). In Taiwan as a whole, 71.2% of PCDD/Fs originated from stationary sources. Long-range transport could bring air pollution from the Northern continent or Indochina peninsula to Taiwan depending on the season. Cytotoxic research found that highest concentration of PM_{2.5} does not correspond to high toxicity. About 150% elevation of ROS and positive genotoxicity was observed after exposure with organic compound of cooking samples. Epidemiological research found that higher concentration of PM_{2.5} and PCDD/Fs in the ambient air positively associated with mortality. PM_{2.5} from stationary sources had higher impact on CVD (0.8% increase each $\mu\text{g}/\text{m}^3$ PM_{2.5}) and respiratory diseases mortality (2.0% increase each $\mu\text{g}/\text{m}^3$ PM_{2.5}) comparing to traffic originated PM_{2.5} (0.4% and 0.6% increase respectively).

Keywords: PM_{2.5}, PCDD/Fs, source apportionment, health risk

萜類化合物與古植物學鑑定化石樹脂植物來源

張世正¹、張英如¹

(1)臺灣海洋大學地球科學研究所

化石樹脂是古代的植物分泌物也是琥珀以及柯巴的總稱，經過長時間掩埋、溫度以及壓力作用下所形成的脂狀物，其中萜類化合物組成記錄著植物來源之訊息，可做為化石樹脂之生物指標，故可藉由有機地球化學分析方式，探討其植物來源。本研究利用傅立葉紅外光衰減全反射光譜(Fourier transform infrared - attenuated total reflection spectroscopy, FTIR-ATR)以及熱裂解氣相層析質譜儀(Pyrolysis Gas chromatography-mass spectrometry; PY-GC-MS)分析來自拉脫維亞、緬甸、馬達加斯加、多明尼加以及印尼之化石樹脂。FTIR-ATR 的初步成果顯示於 2955 cm^{-1} 以及 2870 cm^{-1} 甲基以及亞甲基的對稱收縮訊號， 1700 cm^{-1} 有來自醛、酮的 C=O 拉伸的訊號， 1600 cm^{-1} 則為 C=C 官能基訊號， 1451 cm^{-1} 以及 1385 cm^{-1} 則有來自環己烷甲基之 C-H 鍵的彎曲震動， 1150 cm^{-1} 到 1050 cm^{-1} 有 C-O 伸縮震動且拉脫維亞在此有一特徵峰 “Baltic shoulder”，馬達加斯加的樣本於 887 cm^{-1} 則有 exocyclic methylene。PY-GC-MS 的初步成果顯示，拉脫維亞的樣本含有顯著 succinic acid 化合物以及 abietan、pimaran 的二萜類化合物(diterpenoid)，植物來源可能為金松科的裸子植物；緬甸的樣本則含有 fichtelite、phyllocladane type 二萜化合物且缺少 labdane，植物來源高機率為南洋杉科；多明尼加以及馬達加斯加則含有 enantio labdane 的化合物，其植物來源可能為被子植物中的豆科植物；印尼的化石樹脂成分含有倍半萜類(sesquiterpenoid)的 cadelene 以及三萜類的 α -amyrin、 β -amyrone，由於缺少二萜類成分，故可推論本研究之印尼化石樹脂其植物來源可能為被子植物中的隴腦香科(Dipterocarpaceae)。本實驗可得知利用萜類化合物以及其官能基鍵結可有效分析化石樹脂的植物來源。

中文關鍵字：化石樹脂、萜類化合物、傅立葉紅外光衰減全反射光譜、熱裂解氣相層析質譜儀

Geochemistry of pore water around the Keelung Submarine Volcano, off northern Taiwan and its hydrothermal implication

Feng-Hsin Hsu¹、Chih-Chieh Su¹、Hsio-Fen Lee²、Yu-Shih Lin³、
Song-Chuen Chen⁴、Yunshuen Wang⁴

(1)Institute of Oceanography, National Taiwan University、(2)National Center for Research on
Earthquake Engineering, National Applied Research Laboratories、(3)Department of Oceanography,
National Sun Yat-sen University、(4)Central Geological Survey, Ministry of Economic Affairs

The Keelung Submarine Volcano (KLSV), located in the near-shore area of northern Taiwan, is the seaward extension of the Northern Taiwan Volcanic Zone, with most of the gas emissions concentrate around the northern border of the volcanic cone. In this study, we focused on the geochemistry of pore water with two sediment cores collected from both northern and southern borders of KLSV. Results showed that they were not only characterized by gas enrichment, but also revealed specific geochemical features of pore water, implying a significant influence of hydrothermal fluid. The elevated DIC and TA, lowered pH, and much heavier $\delta^{13}\text{CDIC}$ implied the high flux of volcanic CO_2 input. The downward decreasing of Mg^{2+} (<5 mM below 120 cm) and Cl^- (< 200 mM below 120 cm) in pore waters indicated an obvious mixing between seawater and hydrothermal fluid relative to the phase separation reaction. Based on two end-member mixing model of Mg^{2+} , the highest fraction of hydrothermal fluid is estimated to be 92.2%. Furthermore, extremely high concentrations of Li^+ were observed in pore waters (>2.0 mM), which means the sampling locations are related to high-temperature (>350 °C) rock/sediment-fluid interaction. The end-member values of volcanic fluid are estimated to be 2.12~3.35 mM with an average of 2.52 ± 0.29 mM, which is close to the estimates of hydrothermal field in the Okinawa Trough. All the geochemical results in pore water reflected the importance of secondary modification processes after high-temperature water-rock interaction, especially the interaction between hydrothermal fluid and sediment.

Keywords: Keelung Submarine Volcano, sediment-hosted hydrothermal system, pore water

新竹客雅溪 2017 年河水與底泥汙染物質的時空分佈

魏國彥¹、黃許麗娟²、顏春蘭³

(1)臺灣大學地質科學系、(2)工業技術研究院綠能與環境研究所、(3)環保署環境檢驗所

客雅溪流經新竹科學園區與新竹市區，環保署為監測工業排放與生活污水的汙染潛勢在 2017 年分三次採集該溪河水與底泥，進行主次要與微量元素的分析，並對結果做主變量分析，從 55 個水與底泥標本中辨識出四個相似的元素組合，各組合依序解釋了多變量數據資料中的最大量變方，其百分比依序大約為：38%、20%、15%、7%。其元素組合、分佈及意義分述於下：

第一組合（鉍、鈷、鐵、鎳、鈇）解釋了最大量的數據變方，時空分佈也最廣，暗示有汙染源存在於客雅溪上游與下游，而河川出海口的底泥有較高含量的此組合元素暗示河口的污水處理廠處理未完全，仍有汙染潛勢。

第二組合（銅、鎳、汞、鎳、磷、鎳、鎢、鈷、鈦）以銅、鎳為最大宗，主要分佈於中、上游，暗示來自客雅溪上游與南門溪的工業。

第三組合（硼、鋰、鋇、鈣、銀）指出現於河川中游的底泥，推測與該地的紙廠早年排放有關。

第四組合（錫、鋅、鈷、鎳）只發現於中游的頂點區域，暗示來自鳳凰橋以上更上游的工業排放，且與新竹科學工業園區無關。

2017/10/11 科學園區可能排出鈷 In、錫 Sn（第四組合元素）。同日中山橋水樣亦含較高之銅 Cu、汞 Hg、鎳 Ni、磷 P（第二組合），可能係生活廢水及其他汙染源所造成。兩者分別暗示科學園區及其他廠商/廢水處理廠商可能利用 10 月 10 日國定假期執法空窗期偷排廢水。

2017 年客雅溪雖出現各汙染物質，但其濃度並未超出河川水水質與底泥品質的管制標準，表示只有輕度汙染。

上述這一套在定點、不定期採集河水與底泥標本進行化學與統計分析的方法不失為一個監測工業都市河川汙染的良好方法。

中文關鍵字：重金屬、都市河川、汙染監測、主變量分析

印尼爪哇西部新生代火山岩之年代學與地球化學特徵

梁瑋琪¹、賴昱銘¹、李皓揚²、辛怡儒³、Ledyantje lintjewas¹、
Iwan Setiawan⁴、Long-Xiang Quek¹

(1)臺灣師範大學地球科學系、(2)中央研究院地球科學系、(3)臺灣大學地質科學系、
(4)Research Center for Geotechnology, Indonesian Institute of Sciences (LIPI)

東南亞地區位於三大板塊，歐亞板塊、菲律賓板塊和印度—澳洲板塊聚集邊緣的交匯處，同時也包含了數個活躍的板塊隱沒帶，並有著許多由早期岡瓦納古大陸(Gondwana)分裂的地殼，歷經古生代至新生代的地質構造活動後聚集至現今東南亞位置。爪哇島位於巽他古陸(Sundaland)的南緣，為一平行於巽他-班達隱沒帶(Sunda-Banda Subduction Zone)之島嶼，依照大地構造的分布可分為西瓜哇、中爪哇、東爪哇三個地塊。西瓜哇以新生代火山島弧為主，其北部為巽他古陸大陸基盤，中、東爪哇以白堊紀增積的蛇綠岩體及島弧岩石為主，南部殘存的部分太古代大陸地殼則平行分布於爪哇全島。針對西瓜哇研究的部分，前人在定年工作上有數個第三紀的鉀氫定年結果，並初步討論新生代火山在空間上的分佈；地球化學部分，前人工作僅有全岩主要元素的分析，因此本研究將於西瓜哇地區採樣並進行了更詳細的定年與地球化學分析，從而試取得西瓜哇地體演化架構相關線索，以及西瓜哇各期火山活動之年代。

本研究於西瓜哇採集了新生代之火山岩（共 55 個），並依照火山和地理位置把樣本分成五群(Danau 火山體、Bayah Dome 北部、Bayah Dome 南部、Gede 火山體、Ciemas 火山體)，進行鋯石鈾鉛定年分析與全岩地球化學分析。鋯石鈾鉛定年初步結果可將西瓜哇的火山岩分兩期，分別為中期中新世(11~17 Ma)到晚期中新世(5.4~9.9 Ma)及更新世(小於 1 Ma)。空間上的分布：中期到晚期中新世出露在整個 Bayah Dome 地區(南、北部)；更新世火山岩為整個西瓜哇最年輕的火山岩體，主要出露在 Danau 火山體、Bayah Dome 北部和 Ciemas 火山體；從初步結果可得知第三紀的岩漿活動具有由西瓜哇南部向北部，呈現年代愈趨年輕的現象並呼應前人使用鉀氫定年結果之相同推論。另外，在 Bayah Dome 北部具有白堊紀年代約 140 Ma 之繼承鋯石紀錄，並可對比至蘇門答臘同時期的岩漿活動，顯示此岩漿活動由蘇門答臘南延至西瓜哇北部。全岩地球化學中，主要元素指出此區域火山岩主要為鈣鹼質的玄武岩至石英安山岩 ($\text{SiO}_2 = 45\sim 69 \text{ wt.}\%$)；微量元素部分，輕稀土元素對重稀土元素有相對較富集的現象和微鎔負異常，並且呈現高場強元素(high field strength elements, HFSEs) 虧損，特別是鈮、鉍及鈦(TNT)等元素，以及大離子親石元素(large ion lithophile elements, LILEs)富集，呈現典型的島弧岩漿地球化學特徵。

本研究發現印度—澳洲板塊在西瓜哇地區呈現多階段的隱沒作用，並可將島弧火山的空間分布與噴發時間相聯結，地化部分還有待後續的全岩鋇釷同位素與鋯石鉛同位素資料獲得後，做更進一步的岩石成因的探討。

中文關鍵字：印尼爪哇、巽他島弧、新生代火成岩、鋯石鈾鉛定年法、全岩地球化學



印尼西瓜哇碎屑鋯石及繼承鋯石之鈾-鉛定年學研究

羅琳¹、賴昱銘¹、李皓揚²、辛怡儒³、Iwan setiawan⁴、
Lediyantje lintjeras¹、Andrie Al Kausar¹、Long Xiang Quek¹

(1)臺灣師範大學地球科學系、(2)中央研究院地球科學研究所、(3)臺灣大學地質科學系、

(4)Research center for geotechnology, Indonesian Institute of Sciences

爪哇島位於中生代巽他大陸核心的邊緣，是一平行隱沒帶之東西向島嶼。印澳板塊自中生代起開始向北漂移，並隱沒至歐亞板塊下方，形成多次的隱沒作用，期間也曾發生微板塊貼合事件，造成爪哇島由東向西之地體架構有所不同，依照其特徵可將爪哇島分為西瓜哇、中爪哇和東爪哇。西瓜哇北部的火成活動，為蘇門答臘向東延伸的白堊紀火山島弧，其他區域則以新生代火山島弧為主，火山活動年代包括第三紀及第四紀至今。前人針對西瓜哇 Jatibarang 地層與南蘇門答臘出露之火成岩進行研究，發現兩者具有相似的岩性與特徵，但並未提出年代的證據。本研究於西瓜哇採集砂岩（包括海砂），進行鋯石鈾-鉛定年分析，並搭配火成岩中分析所得的繼承鋯石，依據鋯石年代在時間與空間上的分布情形，試取得西瓜哇在不同時期之鋯石來源區域，以及西瓜哇各期火山活動之年代。

本研究共分析 5 個砂岩，分別採自 Ciemas 及 Cihara；以及 1 個位於 Bayah Dome 沿海的海砂樣本，總計 596 顆鋯石；並於 Danau 火山、Karang 火山及 Ciletuh 灣區採集的 3 個火成岩中，挑選繼承鋯石共 62 顆。目前年代分析結果指出：(1) 西瓜哇西北部具有約 140 Ma 之鋯石紀錄，可與蘇門答臘同時期的岩漿活動年代做對比，此年代並未見於西瓜哇南部樣本。(2) 西瓜哇新生代以來之岩漿活動，具有遠離隱沒帶越趨年輕的現象，由南向北分別記錄到 25 Ma、17 Ma 及 11 Ma 三期事件。(3) 本研究於 Cihara 和 Bayah Dome 的砂岩及海砂中獲得始新世、白堊紀和三疊紀之碎屑鋯石訊號，結果顯示物源分別來自蘇門答臘、施瓦納山脈及錫帶花崗岩。

中文關鍵字：碎屑鋯石、鋯石鈾鉛定年學、西瓜哇、巽他島弧、新生代岩漿活動

Linking K-feldspar $^{40}\text{Ar}/^{39}\text{Ar}$ geochronology with textures and compositions

Yu-Ling Lin¹、Tung-Yi Lee¹、Ching-Hua Lo²、Sarah C. Sherlock³、
Yoshiyuki Iizuka⁴、Tadashi Usuki²、Long-Xiang Quek¹、Punya Charusiri⁵

(1)Department of Earth Sciences, National Normal Taiwan University、(2)Department of Geosciences,
National Taiwan University、(3)School of Physical Sciences, Faculty of Science, Technology,
Engineering and Mathematics, The Open University, Milton Keynes, United Kingdom、(4)Institute of
Earth Sciences, Academia Sinica, Taiwan、(5)Department of Geology, Faculty of Science,
Chulalongkorn University, Thailand

K-feldspar $^{40}\text{Ar}/^{39}\text{Ar}$ geochronology has drawn a lot of attention for its moderate closure temperature in thermal history reconstruction and common occurrence in most lithologies. However, the complexity of K-feldspar $^{40}\text{Ar}/^{39}\text{Ar}$ step heating age spectrum raises difficulties in its age interpretation. The two plateau-like segments shape, one type of the K-feldspar spectra, was inferred as the result of excess argon contamination in the past. This study finds an alternative plausible scenario for such spectrum shape through petrologic and EPMA analyses on K-feldspars in a sheared leucogranite sample from the Mae Ping shear zone, NW Thailand. This leucogranite had rounded and fractured perthitic K-feldspar phenocrysts embedded by albite, and the largest grain can be up to 3 cm in length. Fine-grained K-feldspars at the pressure shadows and boudin necks of albite fishes have distinct textures and chemical compositions from phenocrysts. Two-feldspar thermometers suggest lower equilibrium temperatures of 266°C for the K-rich fine-grained K-feldspar, and higher equilibrium temperature around 373°C for Na-rich phenocrysts. Modeling with multi-diffusion size extractor indicates a high closure temperature of 350°C for the old, high temperature segment while a low closure temperature of 160°C for the young, low temperature segment. Therefore, the K-feldspar $^{40}\text{Ar}/^{39}\text{Ar}$ age spectrum with two plateau-like segments may result from the two major distinct diffusion domain sizes associated with Na-rich phenocrysts and K-rich recrystallized fine grains.

Keywords: K-feldspar, $^{40}\text{Ar}/^{39}\text{Ar}$ dating, EPMA, diffusion domain, closure temperature

Age and geochemical characteristics of the Cenozoic volcanic rocks in Pacitan area, East Java

Ledyantje Lintjewas¹、Yu-Ming Lai²、Iwan Setiawan³、Hao-Yang Lee⁴、
Andrie Al Kausar¹、Yoshiyuki Iizuka⁴、Long-Xiang Quek²

(1)Department of Earth Sciences, National Taiwan Normal University; Research Center of Geotechnology, LIPI, Indonesia、(2)Department of Earth Sciences, National Taiwan Normal University、(3)Research Center for Geotechnology, Indonesian Institute of Sciences、(4)Institute of Earth Sciences, Academia Sinica, Taiwan

The subduction of Indian-Australian oceanic crust beneath the Eurasian plate produced the Cenozoic volcanoes on Java Island at the SE Sundaland. Two Cenozoic arc chains are identified on Java: The Late Eocene-Early Miocene volcanic arc that formed the Southern Mountains known as the 'Old Andesite'; another is the modern volcanic arc that has been active since the Late Miocene and erupted in the central part of Java Island. The Pacitan area is a part of the Southern Mountains, and this study focuses on the volcanic rocks in this area to recognize the magmatic stages and identify the geochemical variations from different stages. We identify two magmatic period in the area, Late Oligocene (26.0-26.7 Ma) and Middle Miocene (12.0-13.0 Ma) using the zircon U-Pb method. Our age results are younger than the previous results from the K-Ar method (28 Ma and 15-19 Ma, respectively). The Late Oligocene volcanic rocks vary from andesite to dacite, and are comparable to medium to low-K calc-alkaline volcanic rocks. The Middle Miocene volcanic rocks vary from basalt to dacite, and comparable to high-K calc-alkaline to tholeiitic volcanic rocks. Nb/U–Nb, Ce/Pb–Ce diagrams, and the depletion of HFSEs (Nb, Ta, and Ti) shows arc characteristics in these volcanic rocks. The LILEs (such as Cs and Rb) and Pb enrichment in the Late Oligocene rocks are significantly lower than those in the Middle Miocene rocks. These results may be because of the different effects of the subduction-related fluids between these two stages in Java Island.

Keywords: Java island, Southern Mountain, Cenozoic magmatism, Old Andesite, Zircon U-Pb dating.

The role of fluid drainage in fault slip zone during earthquake propagation

Nguyen Thi Trinh¹、Li-Wei Kuo²

(1)Department of Earth Sciences, National Central University、(2)Department of Earth Sciences, National Central University; Earthquake-Disaster and Risk Evaluation and Management (E-DREaM) Center, National Central University

Clay gouge is a common material in the brittle fault slip zone. Because of its low frictional strength, clay gouge plays as an important role in controlling the frictional strength of slip zone during the movement, e.g., earthquake propagation or landslides. The host rock adjacent to the slip zone can be either conduit or barrier for fluid flow during fault movement, yet the effect of fluid drainage on fault strength (behavior) is still poorly understood. To understand the effect of fluid drainage on the frictional strength of slip zone, we conducted rotary shear rock friction experiments on water-saturated kaolinite gouge under undrained and drained conditions. In addition, we use two kinds of filter paper to simulate different efficiency of fluid drainage under drained conditions. All experiments we conducted at a normal stress of 10 MPa and a slip rate of 1 m/s with total displacement ~5-7 m. The results show that (1) under undrained conditions, the friction coefficient (the ratio of shear stress/normal stress) achieves a peak value of 0.30 ± 0.01 then dramatically decreases to a steady-state value of 0.18 ± 0.02 associated with sample dilatancy. Under drained condition, the friction coefficient achieves peak values ranging from 0.28 ± 0.01 to 0.30 ± 0.01 , dramatically decreases to steady-state values of 0.21 ± 0.01 to 0.22 ± 0.01 , and then gradually re-strengthens with slip with sample compaction; (2) the slip-weakening distance D_c is varied from 2.03 ± 0.52 to 2.22 ± 0.49 under undrained and high-efficient-drainage conditions, respectively, to 1.14 ± 0.51 under less-efficient-drainage condition. After shearing, the color of kaolinite was changed from white to grey-dark color, and slicken-side textures were only observed on the slipping surface under drained condition. These results suggest that gouge was suffering frictional heat under drained condition, likely resulting from flash heating occurred on the slip surface.

Keywords: frictional behavior, fluid drainage, rotary shear, kaolinite, flash heating

Natural and experimental evidence of deformation on serpentinite

Wei-Hsin Wu¹、Li-Wei Kuo¹

(1)Department of Earth Sciences, National Central University

Serpentinite is regarded as a controlling factor for the nucleation and propagation of earthquakes within subduction zones. Recently, we have provided the evidence of deformation within serpentinite and nephrite from the paleo-subducting-origin Yuli Belt, Taiwan. However, the associated deformation conditions of which remain unclear. This study performs low-to-high velocity rotary shear (LHVR) rock friction experiments on water-saturated serpentinite gouges (sieved for grains size under 0.125mm) to investigate the frictional behaviour of incohesive serpentinite and the associated microstructures. All samples are deformed at either sub-seismic (0.001m/s) or seismic slip rates (1m/s) under both drained and undrained conditions at 10-MPa normal stress and ~5-m slip. Results show that the apparent friction coefficient μ is influenced by water drainage regardless of slip rates. For undrained condition, μ increased up to a peak value $\mu_p \sim 0.32-0.46$ and reached low steady-state value $\mu_{ss} \sim 0.2$, exhibiting a pronounced weakening behaviour explained by pore pressure rise. In contrast, under drained condition μ showed stable sliding ($\mu \sim 0.2-0.3$) or strengthening ($\mu > 0.2$) behaviour. Microanalytical methods, including optical microscope, field emission scanning electron microscope and in-situ synchrotron X-ray diffraction, will be utilized for the LHVR experimental products in near future. These mineralogical and microstructural results could provide a plausible mechanism for the obtained frictional behaviour. In particular, by integrating the recently reported deformation evidence of serpentinite, our results might help to determine the deformation modes within the serpentinite shear zones, and that the signatures of either transient frictional heating by propagation or pressure solution by creep were preserved in the studied serpentinite and nephrite of the Yuli belt.

Keywords: serpentinite, rotary shear, rock deformation, Yuli Belt

Crystallographic orientation-dependence of Raman mode behavior in ortho-(Mg, Fe) SiO₃ single-crystals under pressure

Sheng-Chih Chung¹、Florian T.S. Hua¹、Jennifer Kung¹

(1)Department of Earth Sciences, National Cheng Kung University

The major constructed unit for the pyroxene structure is the linkage of silicon-oxygen tetrahedrons (SiO₄) to form continuous chains. The chain structure reflects on the Raman pattern to be two strong paired Raman peaks (doublet) at the range of 660 and 1000 cm⁻¹, thereafter marked as 'D1' and 'D2', respectively. Previous Raman observations of pyroxenes indicated the doublet of 660 cm⁻¹ (D1) being sensitive to symmetry change, no matter induced by applied pressure or composition changed. In orthopyroxene, composition of (Mg, Fe) SiO₃, lately high pressure X ray diffraction studies showed that this series of pyroxene has a new high-pressure phase, HP P2₁/c. While the mentioned above phase transition occurred, the doublet of 660 cm⁻¹ (D1) would split into triplet from previous studies. Such observation has become a characteristic feature of symmetry changed from Pbc2₁/c to HP P2₁/c. However, those observations were carried out either in powder form sample or unorientated single crystals. In order to investigate the detailed Raman mode feature of orthopyroxene across the phase transition, we measured the changes of the Raman modes, D1 and D2, along different major crystallographic axis, a, b c and face (210), up to 20 GPa. The composition of tested orthopyroxene ranges from Mg#100 to Mg#92, which the phase transition pressure of Pbc2₁/c @ HP P2₁/c should be higher than 10 GPa. From a series of Raman measurement, we found the doublet splitting only observed on "c" axis. Moreover, in this study, both D1 and D2 were observed the splitting. Most strikingly the doublet splitting occurred as low as 4 GPa in which the pressure is far away from the phase transition defined by X ray diffraction. Our results raise the question if the doublet splitting in D1 and D2 can used as the sign of phase transition of orthopyroxene any longer. In this meeting we will report and discuss the observation in details.

Keywords: high pressure, Raman, pyroxene, phase transition

Discretized Clay Shell Model (DCSM) of clayey Sandstone: Evaluating the effective stress coefficient of permeability

Pin-Lun Tai¹、Jia-Jyun Dong²

(1)Graduate Institute of Applied Geology, National Central University、(2)Graduate Institute of Applied Geology, National Central University; Earthquake-Disaster and Risk Evaluation and Management Center, National Central University

The effective stress coefficient determines the effective stress, which dominating the permeability of rocks. However, the documented value of for rocks shows a high scatter (0.3-5.5), based on the laboratory measurement. The well know Clay Shell Model (CSM) successfully explain why the effective stress coefficient of the clayey sandstone can well above 1 theoretically. However, CSM cannot account for the stress dependency of effective stress coefficient observed experimentally. In this study, a modification of CSM was proposed. This proposed Discretized Clay Shell Model (DCSM) discretizes multi-layers clay domain to account for the stress dependent elastic modulus of clay and calculates the pore radius of DCSM model under different confining stress and pore pressure. Iso-pore radius curves under different confining stress and pore pressure was used to determine the effective stress coefficient. The parametric study illustrates the superior features of the proposed DCSM to the traditional CSM. Critical findings include: (1) The predicted effective stress coefficient form a concaving upward surface in the pore pressure-confining stress space using DCSM. (2) The influence of pore pressure on effective stress coefficient will be stronger than the influence of confining stress especially under low pore pressure. (3) The predicted effective stress coefficient is not necessary positively or negatively correlated to confining stress under constant pore pressure. (4) The predicted effective stress coefficient for soft, high stress dependent deformability of clay coating on the pores of sandstones could be far higher than 1. Two synthetic cases (laboratory and in-situ scale) illustrate the importance of stress dependent effective stress coefficient for determining the effective stress and permeability.

Keywords: permeability, effective stress coefficient, clayey sandstone

Rock physics parameters estimations of gas-hydrate and free gas concentrations in Formosa Ridge, Offshore SW Taiwan

Dipika Anggun Ardiantl¹、How-Wei Chen¹

(1)Department of Earth Sciences, Inst. of Geophysics, National Central University

Rock physics parameters usually can be estimated through well log-based analysis approaches with various proposed models and empirical equations. We propose a strategy which treat seismic data as a pseudo-log then combine post- and pre-stack modeling and inversion efforts for rock physics study. The approach helps to identify gas hydrate, free gas and its host lithology with fluids existence in Formosa Ridge Off., Southwestern Taiwan. We developed four steps workflow. First, we refined velocity model suggested from conventional NMO stack with semblance analysis. Second, the synthetic CMP gathers are created by reflectivity and convolutional approach respectively. If synthetic and real gather are fit in both offset domains, then confirms the estimated parameters. Third, initial impedance model derived from convolutional and reflectivity method are used separately in post- and pre-stack procedure. Once we have the P- S-impedance model and source wavelets extraction from offset-dependent dataset, then post- and pre-stack inversion were implemented sequentially to extract the best resolvable models. Pre-stack inversion based on three assumptions (a) linearized approximation for reflectivity, (b) angle-dependent Fatti's equation and (c) linear relationship among P-, S-impedance and density. The inferred basic parameters including V_p , V_s and density are the key efforts for further rock physics estimations. The parameters including porosity, bulk-shear modulus, resistivity, and water saturation for understanding the lithology conditions can be obtained through empirical equations. The results can assist us to evaluate the interrelationships among the derived parameters through cross-plots and delineate the potential gas hydrate and free gas concentration zones. The proposed approach enables us to obtain petro-physical properties with the hope that additional feasibility evaluation and confirmation from borehole data will be available in the future.

Keywords: seismic inversion, post-pre-stack, rock physics, gas-hydrate, free gas, pseudo-logs

Petro-physical properties identification of gas hydrate and free-gas in Yuan-An Ridge, southwest Taiwan

Dwi Ayu Karlina¹、How-Wei Chen¹

(1)Department of Earth Sciences, National Central University

Hydrate and free gas existence in the unconsolidated marine sediments produce significantly large effect on the elastic properties changes in Yuan-An Ridge. Simultaneous Prestack Inversion (SPI) were used to distinguish the physical properties changes. SPI use conjugate gradient matrix inversion method in junction with computing angle-dependent reflectivity responses which follows Fatti's equation. Hence, quality control on SPI result by comparing synthetic to real data in angle gather is very important. SPI has two assumptions. First, the constant ratio of S-wave velocity over P-wave velocity within a rock layer and the background trend should corresponds to wet clastic. V_p/V_s ratio is later converted to natural logarithm P-Impedance (Z_p) and S-Impedance (Z_s). Second, based on Gardner equation, natural logarithm of density has linear relationship with P-impedance. Hence, the synthetic responses is computed by reflectivity method defined by the combined effects from P-impedance, S-Impedance, and density. Consequently, the elastic properties including V_p , V_s , density, Z_p , Z_s , V_p/V_s ratio can be obtained. Other associate elastic properties such as P-wave modulus, shear modulus, Young modulus, Bulk modulus, Poisson's Ratio, $\lambda\rho$, and $\mu\rho$ can be derived through known models and its corresponding equations. The parameters to characterize gas hydrate and free gas in unconsolidated marine sediment can be derived through the approach demonstrated. Parameters which are very sensitive to the gas hydrate and free gas existence in Yuan-An Ridge are $\lambda\rho$, and $\mu\rho$. They can be separated from background trend through cross plot.

Keywords: elastic properties, free gas, Fatti's equation, gas hydrate, and incident angle

Toward a realistic lattice solid model for earthquake micro-physics and earthquake cycle simulation

How-Wei Chen¹

(1)Department of Earth Sciences, National Central University

A realistic numerical simulation model for all physical processes underlying the earthquake phenomenon on HPC's would provide a powerful tool to study fault behavior and earthquake nucleation. The microphysical particle-based Lattice Solid Model (LSM) currently being developed at QUAKES provides a basis on which to construct such a model. Presently, the model simulates stress transfer, seismic waves, fracture, friction, heat and gouge dynamics. Simulations show numerous features compatible with laboratory and field studies including shear localization, low-strength faults compatible with the Heat-Flow Constraint, slip pulses on faults, Gutenberg-Richter power law statistics and cycles of seismic activity exhibiting accelerating energy release prior to large events. Ultimately, when fully developed, it is envisaged that the LSM will be capable of simulating all physical processes underlying earthquakes including lubrication and dynamics of fluids, phase transformations, and chemical effects as well as all observable signals including strain, seismic, electric and magnetic. Increased computational capacity, a model refinement process involving feedback with laboratory and field observations, and integration with macroscopic simulation models would provide the means to study the earthquake cycle, and hence, to develop earthquake hazard quantification and forecasting methodology that best uses the incomplete recorded and incoming data. Recent LSM simulation results of patterns of accelerating energy release prior to large events suggest that earthquake statistics can evolve in a predictable way. These results demonstrate the potential utility of realistic numerical simulation models as a means to probe the earthquake cycle, and provide encouragement that earthquake forecasting is feasible, at least under certain conditions.

Keywords: Lattice Solid Model, rupture simulation, micro-physics, earthquake cycle

探討綠島公館鼻安山岩磁特性

詹定騰¹、陳燕華、洪崇勝²

(1)成功大學地球科學系、(2)中央研究院地球科學研究所

綠島為北呂宋島弧的一部分，綠島大部分的岩體是由安山岩熔岩流與集塊岩所組成，偶有凝灰岩地質及碎屑岩流。本研究之樣本為綠島本島北方公館鼻 (22°40' N, 121°29' E) 的安山岩，外觀具有角閃石斑晶組織與深灰色基質，岩石硬度高深灰色岩體，為火山熔岩流產狀。經巨觀磁力(即殘磁)量測發現，該地點在距離不到 100 公尺的兩處露頭 GN163 (22°40'44.31" N, 121°29'27.12" E)與 GN168 (22°40'44.08" N, 121°29'27.01" E)，其古地磁的磁極紀錄正反各異。兩樣本之間有一界線分成上下兩處因此特別採樣。殘磁方向具有正向磁場與反向磁場(兩種磁場方向)GN163 殘磁方向為磁偏角 358 磁傾角 54(正向)GN168 殘磁方向為磁偏角 168 磁傾角-64(反向)，藉由薄片岩象觀察與微量元素分析法，進一步了解是否為不同期火山噴發，或是其他因素而造成古地磁記錄不同。

從 X 光粉末繞射(X-ray diffraction, XRD)與光薄片觀察 GN163 主要礦物為石英(38%)、輝石與閃石(10%)、長石類(30%)；而 GN168 中主要礦物石英(20%)、輝石與閃石(15%)、長石類(45%)；有些許樣本內含有微量黑雲母等特殊礦物(約占 5%)；而樣本中磁性礦物為鐵氧化物(約占 11%)。利用 XRD 特徵峰(35.6° (311))與 X 射線光電子能譜儀(X-ray photoelectron spectroscopy, XPS)(95% 鐵三價，5% 鐵二價)分析樣本所含磁性礦物可能為磁赤鐵礦。在電子顯微鏡(Scanning Electron Microscopy, SEM)觀察磁性礦物，顆粒大小不一最大有 100 μm 上下，最小 2-3 μm，經由能量散射光譜儀(Energy Dispersive Spectrometer, EDS)分析磁性礦物成分，分為兩大族群高鈦(19 wt%)磁赤鐵礦與低鈦(3 wt%)磁赤鐵礦，兩種磁赤鐵礦也都具有微量的鎂和鋁(1-2 wt%)。而在 GN163 與 GN168 皆有觀察到兩種磁赤鐵礦，因此化學成分可能不是影響磁性變化的主因。

而經由地球化學分析稀土元素(rare earth elements)，與未分化鐵質隕石比較，可以發現 GN168 中稀土元素濃度較 GN163 高，因此推論應該為不同期岩漿噴發所致。由於本研究磁性礦物與岩象在公館鼻兩處安山岩岩流並無顯著差異，因此推論造成兩處磁性不同的因素可能為不同期岩漿噴發紀錄所致。

中文關鍵字：綠島、磁性礦物、磁赤鐵礦、稀土元素

Electron microscopic study of smythite as a diagenetic reaction product of pyrrhotite in methane cold-seep sediments from Fengliao Ridge off SW Taiwan

Ko-Chun Huang¹、Wei-Teh Jiang¹

(1)Department of Earth Sciences, National Cheng Kung University

Smythite was considered to have a formula of Fe_3S_4 and a pyrrhotite-like hcp structure intervened by a $b/6$ offset adjoining a vacant octahedral layer very 4 sulfur planes but its composition was subsequently re-determined to be Fe_9S_{11} . In this study, smythite as a reaction product of diagenetic pyrrhotite in cold-seep sediments from Fangliao Ridge off SW Taiwan was investigated by FESEM-EBSD-EDS and HRTEM. Aggregates of platy crystals of pyrrhotite or reacted pyrrhotite were identified in sediments from 7 depth intervals across the sulfate-methane transition zone at 2–3 mbsf of a 5-m sediment core. EDS analyses revealed that the replacement products of pyrrhotite included smythite (Fe_9S_{11}) and domains having smythite-like compositions and EBSD patterns unmatched with the known smythite or pyrrhotite structures. The zone-axis diffraction patterns of the EDS- and EBSD-verified smythite exhibited well-defined $00l$ and even- $h\bar{h}l$ (e.g., $\bar{2}l$) reflections indicating a periodicity of $6C$ (ca. 34 \AA) and odd- hhl (e.g., $\bar{1}l$) reflection rows showing streaking along c^* . Such diffraction features and the periodic $b/6$ offsets of octahedral layers observed in HRTEM images partially supported the early structure model for smythite but were inconsistent with a rhombohedral lattice. In addition to the aforementioned smythite or pyrrhotite diffraction features, the EBSD-unidentifiable smythite-like domains displayed diffraction spots slightly elongated and strong streaking along c^* in the $00l$ and all of the $\bar{h}l$ reflection rows. The results implied that the Fangliao Ridge smythite had a primitive $6C$ structure consisting of three $2C$ units separated by $b/6$ offsets associated with partially occupied octahedral layers. The EBSD-unidentifiable smythite-like domains probably included interstratified layers of smythite- and pyrrhotite-like phases containing partially disordered octahedral vacancies and could be considered a transitional product for the reaction from $4C$ pyrrhotite to smythite.

Keywords: smythite, pyrrhotite, cold seep, electron microscopy, diagenesis

Weathering of rock fulgurite in Kinmen Island, Taiwan

Tze-Yuan Chen¹、Li-Wei Kuo²

(1)Department of Earth Sciences, National Central University、(2)Department of Earth Sciences,
National Central University; Earthquake-Disaster and Risk Evaluation and Management Center,
National Central University

Lightning is one of the most vigorous nature events with the typical energy of 1GJ per strike. Cloud-to-ground (CG) lightning can transmit the carried energy to the target material, resulting in an increase of temperature up to 2000 k. The target materials will (partially) melt and quench rapidly, termed fulgurite. The typical morphology of a rock fulgurite is a dozens-to-hundreds-micrometer-thick dark layer of glass, with the porosity of 5-7 area %, covering on the surface or filling in the pre-existing fractures of the host rock. However, the determination of rock fulgurite is challenging because of the absence of the glassy layer, likely due to weathering. To investigate the weathering of rock fulgurite, this study presents different field occurrences of the fulgurite relict with its remained microstructural and chemical characteristics and develops a field-based glass dissolution model to provide the time constraint. Our recent works have characterized the rock fulgurite formed in 2018, showing the distributed dark area of $\sim 10 \text{ m}^2$. On the exposed surface of the granitic gneiss hill adjacent to the rock fulgurite, several pits with different dark-crust relict ($< 0.1 \text{ m}^2$) were found, showing the consequence of weathering. Our model suggests that the 100-micrometer-thick rock fulgurite glass would take ~ 140 years to be dissolved. Our results imply that rock fulgurites are vastly under-reported due to their vulnerability to destruction and the resulting difficulty in identification. The criteria we propose to distinguish rock fulgurite relict can help to reconcile the observed frequency of lightning with the difficulty in preserving the records of ancient lightning strikes on rocks.

Keywords: Kinmen, lightning, fulgurite, glass, weathering

Raman spectroscopy and thermal conductivity of synthetic pyrope-grossular garnets at high pressure

Han-Yu Chen¹、Yun-Yuan Chang²、Pei-Ying Patty Lin¹、Wen-Pin Hsieh³、
Jennifer Kung⁴

(1)Department of Earth Sciences, National Taiwan Normal University、(2)Institute of Earth Sciences, Academia Sinica, Taiwan、(3)Institute of Earth Sciences, Academia Sinica, Taiwan; Department of Geosciences, National Taiwan University、(4)Department of Earth Sciences, National Cheng Kung University

Garnet is a major rock-forming mineral in the Earth's upper mantle and subducted slab. Knowledge of the thermal properties of silicate garnets is crucial to understand the thermal structure of the Earth's interior. The crystal structure of garnet can accommodate diverse elements. This study aims to investigate the compositional effects on the Grüneisen parameter and lattice thermal conductivity of pyrope (Py, $\text{Mg}_3\text{Al}_2(\text{SiO}_4)_3$)-grossular (Gr, $\text{Ca}_3\text{Al}_2(\text{SiO}_4)_3$) solid solution. The samples used in this study were synthetic single-crystal $\text{Py}_{40}\text{Gr}_{60}$ and grossular. High-pressure Raman spectroscopic measurements of samples were carried out using a diamond-anvil cell. The mode Grüneisen parameter for each observed Raman mode was obtained from the pressure dependence of vibrational frequencies. From the obtained mode Grüneisen parameters, we estimated the thermal Grüneisen parameters of our samples. Besides the Grüneisen parameters, we investigated the influence of Mg/Ca ratio on the lattice thermal conductivity of pyrope-grossular solid solution using time-domain thermoreflectance (TDTR) technique. Our experimental results will help to constrain the compositional effects on the heat flux and thermal structure in the Earth's interior.

Keywords: pyrope, grossular, solid solution, time-domain thermoreflectance, high pressures, lattice thermal conductivity

含水礦物熱導率對隱沒帶震測異常及其地球動力學上之應用

簡祐祥¹、謝文斌²

(1)中央大學地球科學院、中央研究院地球科學研究所、(2)中央研究院地球科學研究所

隱沒作用是將地表物質傳輸至地球內部的重要途徑。大多數的隱沒板塊會經歷蛇紋岩化作用，此過程會透過水合作用將水儲存在含水礦物中，以穩定地傳遞到地函深部。夾帶大量含水礦物的板塊在隱沒過程中隨溫度上升開始脫水作用，這些釋放出的水將會對圍岩的物理性質有顯著的影響。然而，控制隱沒帶溫度變化並觸發礦物脫水的機制目前還缺乏完整的研究。我們將以 MgO-H₂O-SiO₂ 成分系統中橄欖石、蛇紋石、水鎂石的熱導率為例，結合超快速光學與鑽石高壓砧量測礦物於高壓下的熱導率，透過研究含水礦物熱導率的變化如何影響隱沒板塊的溫度剖面，為礦物脫水機制與其對震測觀察中的影響提供新的見解。

我們發現在隱沒至約 200 公里深時，蛇紋石的熱傳導率會受晶體方向性影響，在假設 10 公里厚的蛇紋岩層中產生約 $7 \text{ W m}^{-1} \text{ K}^{-1}$ 的差異，並使板塊中的地溫梯度上升約 50 K。由於蛇紋石的脫水行為對溫度很敏感，這可能會影響到由流體觸發地震的發震位置。部分脫離板塊的蛇紋石塊體，也容易在此深度產生脫水反應並形成該區域的速度異常，此結果將有助於我們解釋 Lehmann 不連續面的成因。此外，由蛇紋石晶體順向排列所形成的低熱導帶也有可能使部分含水礦物能存活至較深的深度，此結果有助於探討地球深部水循環的傳遞路徑。最後，在隱沒到下部地函頂部約 800 公里深處，板塊中由水鎂石富集的區域會分解成方鎂石與液態水，並導致熱導率突然增加約 9-16 倍。此熱導率不連續所造成的板塊溫度異常升高(約 100 K)將改變整體板塊密度與浮力，從而促進板塊滯留在該深度。同時釋出的水也可能遷移並富集在下部地函頂部形成震波低速帶。

中文關鍵字：含水礦物、脫水作用、熱導率、震測異常、隱沒帶

利用名竹盆地的長期地電阻施測估算區域地下水位及

水文地質相關參數

張竝瑜¹

(1)中央大學地球科學系

本研究通過在名竹盆地乾濕季重複進行時序的地電阻測量，推導出各地電阻測量剖面在垂直方向上的相對飽和度和深度變化。藉由 Brooks-Corey 公式估算了地下水位的深度，與可能的比出水率。將鄰近新民觀測井水位的兩處測線所推算水位進行比較後，我們發現使用 Brooks-Corey 公式估算之空氣進入張壓(air-entry suction)的高程，較觀測的地下水位深度的高程平均淺了約 0.5 米。因此在本研究中的所有測站，可根據此一資料進行深度校正得到各測線位置乾濕季地下水位分布及變化。經推算，名竹盆地的地下水位深度約為 6.7 米至 16.7 米。總體而言，乾旱和濕潤季節的地下水位高程均呈現出從上游到下游逐漸降低的趨勢。在 1 月到 3 月的乾季，地下水位的高程因補注量減少而顯著下降。而由 6 月至 9 月主要雨季時間，地下水位高程逐漸上升。但是，如果我們比較由最乾的 3 月進入較濕的 3 月所施測之區域地下水位變化，約在 Min_02，Min_03 和 Min_05 測站附近，存在一南北方向的水位差較低的區域，其幾何分佈大致垂直於河流的方向。而由 Brooks-Corey 公式模型，估算的比出水率約在 0.08~0.16 之間，調查區上游段和濁水溪河道附近地區有較高的比出水率。而單以最乾的 3 月而言，比出水率亦顯示前述的南北向構造，這表明可能存在大致南北方向，導因於集集地震期間斷層活動帶造成的淺部水文地質結構。值得未來加強研究和討論。

中文關鍵字：地電阻、地下水、濁水溪、名竹盆地

土場仁澤地熱區之三維地電阻模型初探

董倫道¹、郭泰融¹、林蔚¹、張佑銓¹、曾振韋¹、林朝彥²、陳棋炫²、
林昶成²

(1)工業技術研究院材料與化工研究所、(2)經濟部中央地質調查所

宜蘭土場仁澤是受矚目的地熱區，民國 60 年代便進行過地熱探勘，並曾經設有小型發電試範系統，後因土石流事件而中斷發電試驗。國內自 2006 年重啟地熱開發以來，土場仁澤地熱區也是重點地熱開發的區域，為瞭解此地熱區的可能地熱構造，本研究進行了寬頻大地電磁探測。測點分布在以土場仁澤為中心，半徑約 5 km 範圍內，共計 32 個測點，涵蓋牛鬥斷層南北兩側地質區，頻率範圍約介於 10 kHz 至 0.001 Hz 間。探測資料經前處理後，使用 ModEM 軟體進行三維逆推，三維模型的地形部份採用海科中心 200 m 的數值模型來模擬地形及海水水體。本研究三維網格的水平間距為 125 m，以模擬起伏地形及側向電阻變化造成的靜態效應；垂直網格間距為 20 m，以降低高頻訊號的模擬誤差；水平及垂直方向三維模型尺寸則分別為 716 km 及 791 km 以降低低頻訊號的模擬誤差。此外，為了降低三維逆推過程的記憶體需求及縮短計算時間，本研究採用非對角線阻抗資料，且每個對數週期擷取 4 個記錄，共選取 28 個頻率作為三維逆推的輸入資料；並採取階段逆推程序，以避免落入局部低區，經反覆測試及運跑後，獲取能符合觀測資料的合理的三維地電阻模型。由初步地電阻模型並參考相關資訊後顯示，熱水可能沿北北東方向導水通道自深部上湧，在土場仁澤地熱區深度約 1 km 內形成約 20 ohm-m 上下的帶狀低電阻區，該低電阻帶的形成推測與熱水換質的低電阻礦物有關，而牛鬥斷層北側的梵梵溫泉亦有類似的帶狀低電阻構造，但兩者間隔著牛鬥斷層，很可能地熱構造並不相連通，但由於牛鬥斷層北側的測點分布不多，故本地熱區詳細的地熱構造，仍有待後續更多資訊之整合後加以評析。

中文關鍵字：土場仁澤、地熱、大地電磁、三維地電阻模型

New approach in multi-scale adaptive mesh construction of 2D/3D Taiwan Models and traveltime tomography

M. Syahdan Akbar Suryantara¹、How-Wei Chen¹

(1)Department of Earth Sciences, National Central University

Traveltime tomography has been used for years. However, low resolution features due to structured mesh system usually prohibit its applicability of accommodating realistic suggestion and potentially large error involved during interpretation stage. Therefore, to avoid this limitations, unstructured adaptive mesh system is needed. A new approach for seismic traveltime tomographic inversion or potentially suitable for other geophysical problems is tested. The goal is to reduce the geophysical uncertainty when merge different types of data which carry various degree of errors while incorporate accurate geographic information into the model. Shortest path ray tracing is implemented for unstructured Delaunay triangulation mesh system. Un-structured mesh system is designed follow Adaptive Mesh Refinement (AMR) scheme with intension to preserve multi-scale features of the model including topography, bathymetry, geological boundary, active fault traces, sensor location and available information of different velocity models. We show that such an unstructured adaptive mesh system can preserve detailed features of 2D Earth surface and then extend to 3D model of Taiwan. The implementation strategy in mesh generation process follow atomic meshing algorithm. Atomic lattice construction algorithm uses designate control points, its density distribution and cell size to perform refinement within particular regions to preserve discontinuous features. Automatic initialization of control points is based on the nominal distance field that derived from the gradient of a particular physical feature such as velocity or topography variations. In the region where the gradient is high, the cell size become smaller than those region where gradient is low. Forward seismic ray tracing for such mesh system also shows better coverage and accuracy. Consequently, incorporate all proposed approaches can produce more reliable traveltime inversion result at the end.

Keywords: unstructured mesh, adaptive mesh system, atomic meshing, seismic ray tracing, traveltime inversion

GPU acceleration on geodynamic simulation via OpenACC

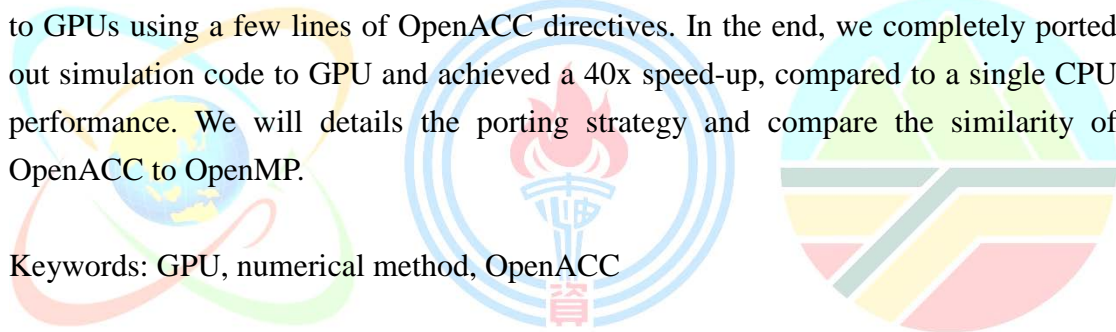
Eh Tan¹、Chase J. Shyu¹、Fang-Yi Lee²、Chih-Chin Lee¹

(1)Institute of Earth Sciences, Academia Sinica, Taiwan、(2)Institute of Oceanography, National

Taiwan University

Numerical simulation on geodynamic processes is computationally expensive. Pursuit of higher resolution and more accurate physical simulation requires more and more computation power. The speed improvement of CPUs has stalled in recent years. Moreover, the speed of memory access has improved only slowly in decades, which further reduces the performance of the simulation. The advance of GPGPU (General Purpose computing on GPU) can help to solve the performance problem. GPU provides quick memory access and fast context switch to hide memory access latency while keeps the computation units busy. Traditionally, the GPU and CPU have separated memory space. Programmers have to transfer data between GPU and CPU manually before and after the computation. The newer generation of Nvidia GPU provides unified memory space to avoid manual data transfers. Additionally, we can port the CPU codes to GPUs using a few lines of OpenACC directives. In the end, we completely ported out simulation code to GPU and achieved a 40x speed-up, compared to a single CPU performance. We will details the porting strategy and compare the similarity of OpenACC to OpenMP.

Keywords: GPU, numerical method, OpenACC



海床絕對壓力計的測試及初步資料分析

林慶仁¹、林豐盛¹、張坤輝¹、許雅儒¹、李炘旻¹

(1)中央研究院地球科學研究所

台灣位處於歐亞板塊和菲律賓海板塊的交界處，台灣東部海域不僅地震頻繁而且板塊聚合的速度也比其他的地方快很多，近幾年來中央研究院也在台灣周圍海域進行了一些使用聲波定位方法進行海床大地測量觀測的研究。為配合海床大地測量觀測，海底絕對壓力測量也是另一種測量的方法。

中研院自製的海床絕對壓力計(absolute seafloor pressure gauge, SAPG)是由 Paroscientific Inc. 出品的振動石英壓力傳感器，配合 RBR-Global Co. 出品的 OEM 資料記錄器 (<http://www.rbr-global.com/products/bpr>) 和 EdgeTech 海底聲納控制電路板…等元件所組成。目前已經完成六部 SAPG 的組裝，有三種不同的外觀設計，並且有 4 部佈放於台灣東部海域進行為期 11 個月的長期觀測。本文將介紹 SAPG 的儀器組裝、出海前的測試及海域資料的初步分析成果。

中文關鍵字：振動石英壓力傳感器、絕對壓力計、大地測量



水下表面波震測施作參數規劃與低頻震源設計初探

林俊宏¹、吳孟哲¹、洪湘詒¹

(1)中山大學海洋環境及工程學系

我國近年來離岸工程的發展越發興盛，由港灣、海纜至風機基礎，乃至於箱網養殖之錨碇，皆與海床之工程性質息息相關，而為有安全穩定之設計，海床的工程性質調查扮演非常重要的角色，影響層面包括場域選擇、興建施工及運維。就現階段之應用而言，海洋地球物理技術主要在規劃階段協助調查工作，除了底床深度調查外，以反射震測類之聲學技術進行底床下之地質狀況調查(如底層剖面儀)為一重要應用，其可定性的顯示底床下方地質之不連續面，配合少數之鑽孔資料協助對地質之判讀，然而此些反射震測類之調查技術無法提供底床之工程性質。水下表面波震測可定量的提供海床之剪力波速，其可直接反映海床之強度、剪力模數、承载力等供地工設計使用之參數。國內目前尚未有相關技術之應用，作者為發展此量測系統，先行透過數值模擬探討水深、土壤參數以及不同施作方法對於水下表面波之行為影響，並據此評估較為合適的試驗系統規格與施作方法，透過數值模擬之初步研究結果顯示，震源應至少能產生最低頻率 5 Hz 之訊號，而接收器亦須至少能接收 5 Hz 之訊號，以收錄到足夠反映底床性質之特徵頻率段；另外，施作中採用定置式地聽器固定於海床上可有最佳收錄效果，若採用水聽器組成之 streamer，則建議離海床最遠不可高於 6 公尺(或是小於所收到蕭特爾波最大波長的 1/4)；而在資料前處理上，當震源遠離海床時，波傳路徑複雜，需將時間域非蕭特爾波的部分濾除可得到較佳之頻散曲線分析成果。而針對低頻率水下震源之開發，初步測試結果顯示，低頻含量與敲擊源之質量有關，質量越高低頻含量越高，將據此進行後續水下低頻震源設計。

中文關鍵字：水下表面波震測、施作參數、低頻震源

勵進南海首航之空氣鎗陣列近場訊號分析

鄧家明¹、林聖心¹、陳鼎仁¹、邱朝聰¹、葉一慶²、許樹坤²

(1)臺灣海洋科技研究中心、(2)中央大學地球科學系

在 2019 年 3 月勵進科學首航航次期間，與國立中央大學地球科學系合作，遠征前往南海中洋脊附近進行研究。在此航次期間，使用約 2 公里 (132 頻道數) 長的受波器浮纜，蒐集約 900 公里長的震測資料，震源系統所使用的空氣鎗為 SECREL 公司出產的 G. Gun II，較方便維護與操作，因此能夠在航次期間為了不同探測目標，在甲板上更換空氣鎗容積配置。此外，雖然空氣鎗容積僅有 1240 in³，但仍清楚的看到沉積層影像中的斷層與基盤等構造。其原因為此震源系統能量較集中，主要透過混合空氣鎗陣列容積與平行鎗簇的方式，提高 P/B (Peak to Bubble) 值，得到更清晰的沉積地層剖面。以南海首航 LGD1901-02 測線的震源訊號資料為例，從分析 4 串鎗簇近場之疊合訊號得知，其 P/B 值約介於 3.84-4.76 之間。進而，模擬遠場之直達波訊號，可發現其氣泡訊號幾乎消失，P/B 值約介於 21.99-32.63 之間。由此可知，此套震源系統能夠有效去除氣泡影響，提供乾淨的訊號。進而，統計此測線的整體 P/B 值，得知 P/B 值集中，67-70% 的 P/B 值落在 1 個標準差值內，且 95% 以上的 P/B 值落在兩個標準差值內，此數據顯示空氣鎗陣列震源訊號品質穩定。因此，使用此分析方式，不僅能夠證明此空氣鎗陣列配置的震源訊號品質，亦希望未來能夠將空氣鎗陣列調整至最佳配置，對於台灣周遭海域能源或地質災害潛勢的調查，提供學研界高品質的震測資料。

中文關鍵字：空氣鎗震源、長支距多頻道震測、勵進研究船

台灣北部貢寮外海之地質構造研究

林怡玟¹、許樹坤¹

(1)中央大學地球科學系

台灣東北海域在造山活動結束後轉為山脈垮塌，而形成一系列東北-西南方向的正斷層構造。而在台灣貢寮地區的逆斷層，澳底斷層、蚊子坑斷層及枋腳斷層似乎與海域上的線型特徵有相關性，推測斷層可能有往外海延伸。為了了解海陸斷層間的關聯，以及這些斷層在海域中是否為活動斷層，使用火花放電反射震測來針對貢寮外海地區做探討，此系統適合淺海區域，且對於淺層構造可以有高的解析度。

在震測剖面中，此區大致上的形貌為東西兩側基盤較高，中間為堆滿沉積物的盆地。資料中可觀察到兩大重點，一是盆地中的沉積層有層序地層的特徵、二是盆地西側邊界的斷層構造。在剖面中可清楚辨識出一侵蝕面，在此不整合面上可觀察到許多水道切蝕填充的樣貌，因其深度大約在 100-200 公尺深，與一萬八千多年前的末次最盛冰期海水面下降 120 公尺左右相近，推測可能為當時所產生的侵蝕面。除此侵蝕面外，也依據震測相的差異定義出沙波基底面、海進面、上一期的最大海泛面及聲學基盤面。而在構造上，可看到一斷距大的高角度正斷層，此斷層有切穿基盤且在近海床的地層也有明顯的錯動。目前懷疑此斷層是因為張裂環境而形成的正斷層斷塊，在斷塊的頂部皆可看到明顯的強反射層。認為這個強反射是在受造山作用影響時，此區域擠壓而抬升，因此在基盤位置堆積了許多粗顆粒的沉積物。後期，造山活動結束改為張裂環境，受沉降作用的影響而形成這些正斷層與盆地。

中文關鍵字：台灣北部海域斷層、火花放電反射震測、層序地層、末次最盛冰期侵蝕面

以反射震測資料探討台灣西南海域南海大陸斜坡之氣窗分布與特性

韓為中¹、陳麗雯²、劉家瑄³

(1)臺灣中油公司探採研究所、(2)海洋委員會國家海洋研究院、(3)臺灣大學海洋中心

本研究藉由分析反射震測資料，探討臺灣西南海域變形前緣西側南中國海大陸斜坡之流體移棲構造分布與特性，由西而東包含九龍海脊、馬蹄鐵海脊、指標海脊及福爾摩沙海脊等 4 個天然氣水合物探勘好景區。震測資料指出本區有密集的海底仿擬反射(BSR)與亮點(bright spots)分布，過往研究亦發現活躍的海床滲漏徵兆，顯示動態的地下流體移棲與聚集特性。研究成果指出除傾斜地層與斷層外，氣窗(gas chimneys)亦是本區重要的流體移棲管道。本研究辨識了共 36 處氣窗，並依其在天然氣水合物儲集系統中所扮演的角色將其分為 2 種類型：第一型氣窗穿過天然水合物穩定帶基底，對於水合物生成甚或海床滲漏有直接貢獻；第二型氣窗則被沉積物深埋，其和水合物生成及海床流體滲漏無直接關聯。此二類型氣窗的空間分布與沉積環境特徵高度相關，暗示沉積作用控制了本區氣窗的發育過程。

中文關鍵字：反射震測、天然氣水合物、氣窗



從地震地層學探討南台灣新近紀以來沉積環境與構造運動之

演變關係

牟敦堅¹、黃瑞澤¹

(1)福爾摩沙能源股份有限公司

近年來台灣有關造山運動時空演化之研究數量很多，依據沉積環境、核飛跡定年、岩屑分析、二次移置化石、前陸盆地構造下沉速率等證據，都不約而同指出台灣的造山運動是在中新世晚期開始，而後在上新世早期抬升加劇。

台灣新近紀的造山運動肇因於菲律賓海板塊與東亞大陸板塊的碰撞。此類劇烈的構造活動，一般都會影響周邊沉積盆地的形貌和沉積環境。原先被動大陸邊緣陸棚上的沉積界面坡度，因碰撞帶地形大幅且快速地抬升而變陡。而突增的侵蝕力，也進而在陸棚外緣與大陸斜坡上深切出海底峽谷。印度板塊在漸新世開始和亞洲大陸發生劇烈的碰撞，巴基斯坦南部印度河口外海域盆地裡的地震剖面上，在漸新統以後的層序裡，經常可見在前置堆積三角洲前緣的深海環境中，存在許多深切的峽谷，這是一個構造運動與沉積環境演變之間因果關係的已知例證。

透過台灣中油公司過去發表的震測資料，讓我們觀察到在海域的台南盆地內，中新統頂部發育有顯著的交角不整合，其後的年輕地層裡，則開始出現深切的海底峽谷與深水相厚層泥岩。陸上的嘉南平原地下，從上新世烏嘴層至更新世中期的崁下寮層，也存在著為數眾多、切深規模數百米以上、唯有在侵蝕基面落差大的大陸斜坡深海環境下，方克生成的峽谷構造。這些地震剖面中看到的地層現象與其對應年代，和前述南台灣造山運動於中新世晚期後加劇的結論基本一致。

中文關鍵字：地震地層學、沉積環境、海底峽谷、造山運動

以 COMCOT-SS 發展印度洋風暴潮系統

曾博森¹、吳祚任¹、林君蔚¹、莊淑君¹、許家鈞¹、莊美惠¹

(1)中央大學水文與海洋科學研究所

印度洋北方之孟加拉地區經常遭受熱帶氣旋侵襲。由於當地沿海人口密度高且多為河流及泥沼地，熱帶氣旋所引致之風暴潮往往對當地造成嚴重破壞。如發生於孟加拉灣之 1970 孟加拉風暴潮，造成近 50 萬人死亡，為人類史上死亡人數最高之熱帶氣旋；2020 年之氣旋 Amphan 與風暴潮事件，亦造成近 13 億美元之損失及 128 人死亡。本研究旨在以台灣 COMCOT 風暴潮預報系統為基礎，發展適用於印度洋之風暴潮速算系統。於印度洋所發展之熱帶氣旋，其結構與強度有別於太平洋之颱風與大西洋之颶風，因此適用於太平洋與大西洋之風暴潮模式是否適用於求解印度洋之熱帶氣旋型風暴潮為本研究之分析重點。本文以 2020 氣旋 Amphan 為研究案例，分析 5 種不同參數化風場與 NCEP 大氣模式於風暴潮生成之適用性，並利用歷史案例（2019 年氣旋 Fani 以及 2013 年氣旋 Phailin）進行模式準確度比較。分析結果發現，修正後之模式(Present Model)模擬之氣象場於風速剖面及時序潮位高程上與觀測資料有最佳之匹配。本研究所採用之 COMCOT 風暴潮預報系統求解球座標非線性淺水波方程式，搭配巢狀網格系統與移動邊界法，可於沿岸求解高解析度之風暴潮溢淹範圍。同時可結合 TPXO 全球天文潮模式，以掌握高低潮位對溢淹範圍之影響。本研究建立適用於孟加拉灣氣旋之 COMCOT 風暴潮速算系統，期待未來對於孟加拉灣地區風暴潮速報及災情掌控有實際之助益。

中文關鍵字：孟加拉灣氣旋、風暴潮、COMCOT 模式、參數化風場

發展 SSIIA 分析法並重建 1845 年雲林口湖風暴潮事件

許家鈞¹、吳祚任¹、林君蔚¹、莊淑君¹、曾博森¹、莊美惠¹

(1)中央大學水文與海洋科學研究所

西元 1845 年雲林口湖發生嚴重之風暴潮事件，造成萬人喪生，為台灣歷史上最嚴重之風暴潮事件。為重建 1845 口湖風暴潮事件，本文發展風暴潮影響強度分析法(SSIIA)。該法以現行於中央氣象局之 COMCOT 風暴潮模式為基礎，進行大量單元颱風之風暴潮模擬，以建立颱風位置對風暴潮與溢淹高程之 SSIIA 敏感關係圖。本研究為重建颱風路徑，發展颱風路徑對風暴潮影響分析法。該法透過 SSIIA 之分析結果，進行風暴潮潮高、溢淹高程與溢淹範圍之綜合評分，以求得可能之颱風路徑組合，並考慮颱風移動速度之差異性，得出最嚴重影響移動速度之路徑，並由該結果建立 1845 年事件之可能情境。透過上述之分析結果，本研究提出對雲林口湖風暴潮生成之颱風情境，以及該路徑所造成之風暴潮和溢淹範圍。本研究所建立之分析方法，可系統性分析沿海低窪地區之風暴潮溢淹潛在災情，有助於進行風暴潮風險評估及災防規劃。

中文關鍵字：風暴潮影響強度分析法 SSIIA、颱風路徑、移動速度、口湖風暴潮、COMCOT 風暴潮模式、風暴潮重建



Coupled OBS and MCS data processing to derive the stratigraphy and velocity of the middle Taiwan Strait

Sebastian Wege¹、Tan-Kin Wang²、Ren-Jie Wei²

(1)Institute of Earth Sciences, Academia Sinica, Taiwan; Institute of Earth Sciences, National Taiwan Ocean University、(2)Institute of Earth Sciences, National Taiwan Ocean University

In the last five years, many seismic datasets were acquired in the Taiwan Strait to understand the shallow stratigraphy of the foreland basin better. Recent seismic activity shows that the area is still active and ongoing offshore construction sites make it worth investigating. Ten ocean-bottom seismometers (OBS) were deployed in June 2017 in an area of 30x30 km and nine multichannel seismic (MCS) profiles were shot using a GI-gun. Supplementary seismic data have been acquired in the northwest of our main profile using two OBS and an MCS system from China. Coupled MCS and OBS data processing was used to make a stratigraphic line interpretation of the shallow sedimentary layers and faults. We picked and inverted refracted and reflected arrivals in the OBS data to obtain a P-wave velocity model consistent with the sedimentary interfaces interpreted in the MCS profiles. We integrated the sedimentary layers of the nine MCS profiles to construct an iso-depth model of the main unconformities. Further, the horizontal components of OBS data have been used to build a Poisson's ratio model. The sedimentary layers above the Break-Up unconformity were cut by nearly vertical normal faults that were occasionally reaching the seafloor. In profile E7 the faults form a flower structure and can hence be identified as part of a strike-slip system. To show the location and direction of the normal faults and strike-slip faults in the area, they have been picked and interpolated across our profiles. The P-wave velocity model has a low-velocity zone or a fracture zone in the northwest, caused by the faults across the basement between Wuchu Depression and Kinmen Rise. Below the Penghu Platform, we found relatively low Poisson's ratios in sedimentary layers caused by the normal faults softening the sediments. Based on the iso-depth model the depth of the Break-Up unconformity gradually becomes shallow from the southeast to the northwest.

Keywords: normal fault, Penghu Platform, Poisson's ratio, P-wave velocity, strike-slip fault, Taiwan Strait, Wuchu Depression

P-wave velocity structures of the sediment and crust across the northern Taiwan Strait imaged by using air-gun and GI-Gun recorded from MCS and OBS data

Sergaud Marseille¹、Sebastian Wege¹、Tan K. Wang¹

(1)Institute of Earth Sciences, National Taiwan Ocean University

In the northern Taiwan Strait, four multi-channel seismic (MCS) profiles with 8 ocean-bottom seismometers (OBS) shot by a GI gun and the northwestern portion of the OBS line shot by strong air guns were collected in 2018. About 60 km NE of 2018 survey area, ten MCS profiles with 6 OBS shot by a GI gun were acquired in 2019. The normal fault at SE side of the northernmost Nanjihtao Basin was identified as the boundary fault between the forebulge and the foredeep. However, most of the normal faults observed from the 2019 MCS profiles were near the central line of the northern Taiwan Strait where the Basal Foreland Unconformity (BFU) was at two-way travel times of 0.52-0.63 s. The northwestern part of the BFU is shallow while it is deep in southeastern part. The 2018 MCS profiles, after intersection with the 2019 OBS line, showed a flower structure generated by the strike-slip faults in the northeastern side of the Kuanyin Platform. On the other hand, the P-wave velocity model inverted from 6 OBS data collected in 2019 indicates a large lateral variation of the P-wave velocity (1.9-2.1 km/s) near the BFU while the P-wave velocity-interface model inverted from 8 OBS data recorded in 2018 shows the increasing thickness of the sediment. P-wave velocities of the upper crust (5-6.5 km/s), the middle crust (7-7.5 km/s) and the lower crust (7-8 km/s) across the Kuanyin Platform are greater than the previous result in the northern Taiwan Strait. However, near the Moho, the P-wave velocity (6-7 km/s) is slower than the previous study. The high-velocity zones of the upper, middle and lower crusts may have resulted in the Littoral Fault Zone NW of the northernmost Nanjihtao Basin near the boundary fault.

Keywords: basal foreland unconformity, faults, forebulge, Kuanyin Depression, Kuanyin Platform